


2017

Opportunities and challenges to use electrical stimulation for enhanced denitrification in woodchip bioreactors

Ji Yeow Law
Iowa State University

Follow this and additional works at: <http://lib.dr.iastate.edu/etd>

 Part of the [Agriculture Commons](#), [Bioresource and Agricultural Engineering Commons](#), [Environmental Engineering Commons](#), and the [Environmental Sciences Commons](#)

Recommended Citation

Law, Ji Yeow, "Opportunities and challenges to use electrical stimulation for enhanced denitrification in woodchip bioreactors" (2017). *Graduate Theses and Dissertations*. 15557.
<http://lib.dr.iastate.edu/etd/15557>

This Thesis is brought to you for free and open access by the Iowa State University Capstones, Theses and Dissertations at Iowa State University Digital Repository. It has been accepted for inclusion in Graduate Theses and Dissertations by an authorized administrator of Iowa State University Digital Repository. For more information, please contact digirep@iastate.edu.

Opportunities and challenges to use electrical stimulation for enhanced denitrification in woodchip bioreactors

by

Ji Yeow Law

A thesis submitted to the graduate faculty
in partial fulfillment of the requirements for the degree of

MASTER OF SCIENCE

Co-majors: Agricultural and Biosystems Engineering; Civil Engineering (Environmental Engineering)

Program of Study Committee:
Michelle L. Soupir, Major Professor
Dave R. Raman
Thomas B. Moorman
Say Kee Ong

The student author and the program of study committee are solely responsible for the content of this thesis. The Graduate College will ensure this thesis is globally accessible and will not permit alterations after a degree is conferred.

Iowa State University

Ames, Iowa

2017

Copyright © Ji Yeow Law, 2017. All rights reserved.

TABLE OF CONTENTS

LIST OF FIGURES	iv
LIST OF TABLES	v
ABSTRACT.....	vi
CHAPTER 1 GENERAL INTRODUCTION.....	1
1.1 Introduction.....	1
1.2 Goal and Objectives	6
1.3 Hypothesis.....	6
1.4 Thesis Organization	7
CHAPTER 2 LITERATURE REVIEW	8
2.1 Impact of Nitrate on Environment, Economic and Human/Animal Health	8
2.2 Transport of Nitrate in Tile Drainage	10
2.3 Denitrification Woodchip Bioreactors	12
2.4 Denitrification Process and Factors Affecting Denitrification Rates.....	15
2.5 Bio-electrochemical Reactors for Denitrification	21
CHAPTER 3 COLUMN SCALE EXPERIMENT	27
3.1 Theory	27
3.2 Material and Methods	29
3.2.1 Overview.....	29
3.2.2 Experimental phase – reactor overview	29
3.2.3 Reactor vessel and packing	31
3.2.4 Electrical stimulation system	32
3.2.5 Fluid handling system	32
3.2.6 Thermal control.....	33
3.2.7 Microbial inoculation.....	33
3.2.8 Sample collection.....	34
3.2.9 Analytical method.....	34
3.2.10 Preliminary technoeconomic analysis.....	37
3.3 Results and Discussions	39
3.3.1 Effect of electrical stimulation on denitrification efficiency	39
3.3.2 Effect of current density on denitrification efficiency and current-denitrification efficiency.....	40
3.3.3 Effect of anode material on denitrification efficiency	42
3.3.4 Factors affecting pH, ORP, and DO and their effect on denitrification efficiency	43
3.3.5 Denitrifying bacterial communities and their role in denitrification.....	45

3.3.6	Technoeconomic analysis	46
3.4	Conclusion	49
3.5	Implication of Work and Future Research.....	49
3.6	Supplementary Data.....	50
APPENDIX A: PRELIMINARY EXPERIMENT		58
APPENDIX B: RAW DATA.....		62
References.....		73

LIST OF FIGURES

Figure 1-1 Schematic diagram of woodchip bioreactor designed to reduce nitrate loading from agricultural drainage into surface water (Christianson and Helmers, 2011).....	4
Figure 2-1: Summary of potential electron transfer mechanisms for denitrification in a bio-electrochemical reactor.....	23
Figure 3-1: Summary of potential electron transfer mechanisms for denitrification in a bio-electrochemical reactor.....	27
Figure 3-2: Exploded view of up-flow bio-electrochemical reactors. Blue arrow represents direction of water flow, which flows from inlet (bottom) to outlet (top) of the reactors. In-Col 1 and 3 are the locations of cathode; In-Col 2 is the location of anode.	31
Figure 3-3: Denitrification efficiency of each treatment at 100 mA (A) and 500 mA (B). SS-C: stainless steel anode-carbon cathode; C-C: carbon anode-carbon cathode	40
Figure 3-4: pH, ORP and DO of each treatment at 100 mA (A) and 500 mA (B). SS-C: stainless steel anode-carbon cathode (dashed line, widest error bar cap); C-C: carbon anode-carbon cathode (dotted line, medium width 50% transparency error bar cap); control (solid line, narrowest 75% transparency error bar cap).	45
Figure 3-5: Comparison on nitrogen removal costs of using electrical approach for denitrification in woodchip bioreactors.....	47
Figure 3-6: Cost breakdown of scenario 1 and 2. Each scenario's assumptions were summarized in <i>Table 3.2</i>	48

LIST OF TABLES

Table 3-1: Summary of operating conditions including current intensity, temperature and hydraulic retention time (HRT) in three respective testing periods. HRT can be obtained by dividing pore volume with flow rate.	30
Table 3-2: Input summary of techno-economic analysis. Interest rate 5%.	38

ABSTRACT

As snow melts in the early spring or during precipitation events in the summer, there is a need to treat larger volume of tile water containing nitrates. However, the size limitation of denitrifying woodchip bioreactors may limit the retention time or quantity of tile water that can be treated during high flow conditions. Lower nitrate removal efficiency in woodchip bioreactors have been observed when hydraulic retention time (HRT) and water temperature are lower. This has encouraged research to improve denitrification efficiency of bioreactors at lower temperature and HRT. One of the potential approaches is to provide an alternative and readily available energy source to the denitrifying microorganisms through electrical stimulation. Previous work has demonstrated the capability of bio-electrochemical reactors (BER) to remove variety of water contaminants, including nitrate, with the presence of soluble carbon source. In this paper, we present the column-scale experiment that was conducted to evaluate the denitrification efficiency of electrically augmented woodchip bioreactors. Three duplicated up-flow column woodchip bioreactors were studied: two controls (non-energized, and without electrodes), two electrically enhanced bioreactors using a 316 stainless steel anode coupled with graphite cathodes, and two electrically enhanced bioreactors using with graphite for both anode and cathodes. Both pairs of electrically enhanced bioreactors have demonstrated higher denitrification efficiency than controls when 500 mA of current was applied. While this technology appeared promising from the perspective of denitrification efficiency, the techno-economic analysis revealed that higher N removal cost (\$/kg N) is needed. This work would serve as the preliminary work to improve the design of electrically stimulated woodchip bioreactors to optimize its performance at lower capital and maintenance costs, and thus lowering its N removal cost.

CHAPTER 1 GENERAL INTRODUCTION

1.1 Introduction

Nitrate in excessive amount poses risks to human health and aquatic ecosystem. Excessive intake of nitrate by human and other warm-blooded animals can lead to a temporary blood disorder called methemoglobin, or more commonly known as Blue Baby Syndrome. Just as the name sounds, infants are more sensitive and vulnerable to this disease due to their high liquid-based diets and lack of enzyme that converts methemoglobin back to its original oxygen-carry form (NHDES, 2006). In addition, nitrate that is converted into nitrite within the human body, is believed to be a cancer-causing chemical to many chronic cancers such as gastric cancer (NHDES, 2006). Nitrate intake by humans generally comes from food and drinking water. Even though drinking water only contributes about 14 percent of the total nitrate intake of an average person, higher values often apply to bottle-fed infants (WHO, 2006). This results in increasing concern of excessive nitrate levels in water bodies, which is mainly contributed by agricultural activities such as application of nitrogen fertilizers. The United States Environmental Protection Agency (U.S. EPA) has set the water quality standard for nitrate-nitrogen in drinking water at 10 mg/L as the safe consumption level to prevent potential human health problems (USEPA, 2014).

The United States Geological Survey (USGS) has evaluated the water quality of aquifer systems, which are water resources to 60 percent of the population in United States, through the National Water Quality Assessment (NWAQA) program. The study has found that 15 percent of the shallow groundwater contains nitrate at concentrations above the safe consumption level (Manassaram et al., 2005). In addition, increasing nitrate levels are observed in many rivers which are tributaries to the Mississippi River. Nitrate concentrations increased by 43 percent and

29 percent, respectively, in the upper Mississippi River and Missouri River between 2000 and 2010 (USGS, 2014).

Nutrients including nitrate that are transported south to the mouth of the Mississippi River have impacted water quality in the Gulf of Mexico. Nutrient enrichment has resulted in the formation of a hypoxic zone, commonly referred as the “dead zone” which was first discovered in 1972 (Melodi and Jason, 2014). In 2008, the EPA Hypoxia Task Force set a goal to reduce the five-year average size of Gulf of Mexico’s hypoxic zone to less than 5,000 square kilometers by 2015. However, the five-year average size of approximately 14,000 square kilometers between 2009 and 2013 shows that it is a difficult goal to achieve within such a short timeframe (Hypoxia Task Force, 2013). In fact, the size of the hypoxic zone was at least 3 times larger (16,760 km²) than EPA’s goal (EPA, 2015).

The application of nitrogen fertilizer and subsurface drainage are common agricultural practices which play an important role in improving agricultural production. However, the application rate and timing can be difficult to be accurately estimated due to the variations in rate and magnitude of nitrogen loss from agricultural field. The uncertainties in nitrogen loss can be affected by combinations of factors, which includes tillage, drainage, crop selection, soil organic matter levels, hydrology, and temperature and precipitation patterns (Dinnes et al., 2002). While subsurface drainage helps to lower the water table or to drain excess water, it also accelerates the leaching process of nitrate through the root zone into tile lines. The nitrate-rich drainage water is usually discharged into local surface waters.

Furthermore, high levels of nitrate in a water body along with the presence of phosphorus can accelerate the process of eutrophication (USEPA, 2012). The increased growth rate of aquatic plants leads to changes in level of dissolved oxygen, temperature and other natural conditions of

water which can essentially alter the aquatic ecosystem (USEPA, 2012). The hypoxic zones around the world have exhibited close relationship between hypoxia and negative impacts on the aquatic ecosystem such as depletion of valuable fish stocks and loss in diversity of aquatic animals (Diaz and Solow, 1999).

The Iowa Nutrient Reduction Strategy (INRS) developed in 2013 aims to reduce non-point source loading of nitrogen by 41 percent (IDALS, 2013). The strategy consists of a change in nitrogen managements, land-use practices, and the implementation of edge-of-field treatment. Some examples of nitrogen managements are nitrogen application rate and timing, and the use of nitrification inhibitor. Meanwhile, shifting from row crops to perennial crops, and introducing crop rotation are considered as land-use practices that would help to reduce nitrate loading. Finally, the edge-of-field treatments include the installation of wetlands, woodchip bioreactors, buffer strips, and controlled drainage.

Woodchip bioreactors are an emerging technology for nitrate removal. This technology is often favored by the farmers because it is an edge-of-field practice which minimizes the amount of land to be taken out of production. The bioreactors which are buried underground, reduce nitrate loading into surface water by routing drainage water through the trench filled with woodchips (Figure 1.1). Meanwhile, denitrification takes place in the bioreactors by denitrifying bacteria which use woodchips as a carbon source. Most of the woodchip bioreactors in Midwest have nitrate reduction efficiency range from 15 to 60 percent, which is slightly less effective than wetlands which can remove 40 to 70 percent of nitrate (Christianson and Helmers, 2011). However, woodchip bioreactors are viewed as a promising technology as it has an advantage over wetland because of their smaller footprint (Christianson and Helmers, 2011). This motivates the development of woodchip bioreactors with higher denitrification efficiency.

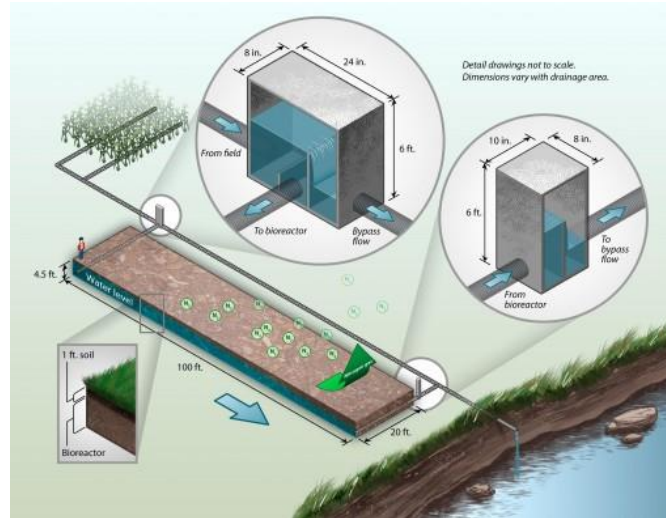


Figure 1-1 Schematic diagram of woodchip bioreactor designed to reduce nitrate loading from agricultural drainage into surface water (Christianson and Helmers, 2011).

Broad variation in environmental conditions and human activities are challenges to design a one-size-fit-all model. In seasonal regions such as the Upper Midwestern United States, which has over 12,841,000 hectares of drained area (Kalita et al., 2007), peak flow occurs during spring when the snow melts. This potentially results in larger influent volume and shorter hydraulic retention time (HRT) in the bioreactors. In addition, cooler water temperature during spring can discourage the microbial activity of denitrifying bacteria and therefore deteriorate the performance of woodchip bioreactors (Feyereisen et al., 2016; Hoover et al., 2015). Consequently, additional research to improve performance of woodchip bioreactors at lower temperatures would be beneficial.

Electrical stimulation of microbial metabolism to remove toxic pollutants including nitrate from wastewater has been practiced for over 50 years (Thrash and Coates, 2008). This technology is also commonly known as Biofilm-Electrode Reactor or Bio-Electrochemical Reactor (BER) and previous studies have exhibited promising nitrate removal efficiency using this approach. For instance, Park (2005) obtained nitrate removal efficiencies of 98% using an applied current of 200 mA to a 2.5 L reactor, with 1 L working volume. Meanwhile, the maximum nitrate reduction

from Park (2005) was 0.17 mg NO₃⁻-N/(cm² (biofilm surface area)-day). On the other hand, Hao (2013) further improved the performance of traditional BER by employing multi-cathode BER, namely 3D-BER. Hao (2013) found that the 3D-BER which has larger cathode surface area was able to increase the removal efficiency from 57.93% (2D-BER) to 78.10% at a 4-hour HRT. Take note that these BERs utilized soluble carbon sources, and this electrical approach has not been tested by using woodchip as a carbon source. In a BER, the nitrate can be reduced biologically or electrochemically (Thrash and Coates, 2008). For biological reduction, the electrons are transferred to the electron transport chain of bacteria to form terminal reductase, which is then used to reduce an oxidized substrate, such as nitrate. Briefly, the electrons can be transferred to the microorganisms in three possible pathways: direct electron transfer from cathode surface, or through electron shuttling using electroactive substrates, or from H₂ produced from electrolysis of water. Alternatively, the electrochemical reduction of nitrate involves the change in oxidation number of nitrate without the use of microorganisms.

The goal of this research project was to enhance nitrate removal efficiency of woodchip bioreactors by introducing electrical stimulation. The nitrate removal efficiency of BER at low temperature condition also will be investigated. This research involves the integration of two technologies - woodchip bioreactors and BER into a new technology. This new management strategy will allow for design of a bioreactor with lower HRT and thus a system which processes higher volume of drainage water at a smaller scale. This will potentially reduce the nitrate removal cost and footprint of bioreactors, which could encourage greater implementation of conservation practices.

1.2 Goal and Objectives

The goal of this study was to improve the denitrification efficiency in denitrifying woodchip bioreactors using electrical stimulation. The objectives of this study were:

- i. To compare denitrification efficiency with and without electrical stimulation
- ii. To compare denitrification efficiency and current-denitrification efficiency at different current intensities
- iii. To compare denitrification efficiency and current-denitrification efficiency by using different anode material
- iv. To observe pH, ORP and DO in all treatments and control
- v. To evaluate the economic feasibility of electrical stimulation

1.3 Hypothesis

The hypotheses of this study were:

- i. Electrical stimulation will enhance denitrification efficiency in woodchip bioreactors
- ii. Abiotic reaction at the electrodes can be affected by the electrode material
- iii. More electrons are supplied using higher applied potential, thus increasing the denitrification efficiency
- iv. Oxidizing and reducing zones are developed at anode and cathodes, respectively

1.4 Thesis Organization

This thesis was organized into three chapters. The first chapter provides an overall introduction, and additional information was detailed through literature review sections in the second chapter. Chapter 3 followed the paper format, and presents all information of the column scale experiment.

CHAPTER 2 LITERATURE REVIEW

2.1 Impact of Nitrate on Environment, Economic and Human/Animal Health

Nitrogen and phosphorus loading from agricultural lands into water bodies are known to cause many environmental problems, including hypoxia in fresh and marine waters. Hypoxia occurs through a series of ecological processes, and the first step in the chain is an overwhelming supply of nutrients to an ecosystem (ESA, 2012). Nitrogen is often considered to be the limiting nutrient in marine waters, while phosphorus is the limiting nutrient in fresh water ecosystem (Howarth and Marino, 2006). This process is also known as eutrophication and when it is combined with multiple environmental factors such as warm water temperatures and poor mixing rates, a favorable environment exists for algal overgrowth, or algal blooms (ESA, 2012). This often occurs in coastal and estuaries areas where water is poorly mixed due to waterbody stratification (saline and temperature gradient) and flux of nutrients from upstream (ESA, 2012). As these overabundant algae die and decompose, the decomposers consume oxygen in the process, which reduces the oxygen levels in water (Mississippi River/Gulf of Mexica Hypoxia Task Force, 2012).

An area is defined as a hypoxia zone when the water at the sediment surface contains DO levels below 2 to 3 mg/L (Mississippi River/Gulf of Mexica Hypoxia Task Force, 2012). This zone is also commonly known as the “dead zone” because of its inhospitable environment for many aquatic species resulted from low dissolved oxygen (DO) levels (Hypoxia Task Force, 2013). Currently, there are more than 400 marine systems around the world with reported dead zones, and these zones are affecting a total area larger than 245,000 square kilometers (Diaz and Rosenberg, 2008). The direct impact from hypoxic waters is decline in population and diversity of aquatic species, especially the immobile animals that cannot escape to waters with higher DO

levels (ESA, 2012). Coastal and estuaries areas are also nursery grounds for many aquatic species. The hypoxic conditions in these areas further destabilized the ecosystem as the adult species are not able to reproduce or the young species are not able to survive. Consequently, substantial overall reductions in fish stocks are observed and fish-eating birds and mammals can no longer live in an area when fish population are decreased or absent (ESA, 2012).

In the United States, the formation of the hypoxic zone in the Gulf of Mexico is driven by nutrients exported from the Mississippi River Basin. The dead zone in Gulf of Mexico is estimated to be one of the largest in the world, covering 5-year average area of 14,000 square kilometers from 2009 to 2013 (Hypoxia Task Force, 2013). This has a significant negative impact on the fishery industry, which accounts for 68% of shrimp landings, 55% of oyster landings and 31% of recreational marine fishing trips in the United States (Karnauskas et al., 2013). National Oceanic and Atmospheric Administration (NOAA) estimated an annual loss of \$82 million from seafood and tourism industries due to poor water quality (The Nature Conservancy, 2011).

In addition to environment and economic impacts, nitrate contamination in drinking water is also a well-known risk factor for several human and animal health issues. In the body, nitrate can be converted into nitrite, and the nitrite can oxidize ferrous (Fe^{2+}) into ferric (Fe^{3+}). Essentially, the conversion of iron in red blood cells alters the function of hemoglobin, which makes it unable to carry oxygen throughout the body (Water Sanitation and Health, 2001). In chronic conditions, lethargy, increase in saliva production, loss of consciousness, seizures and even deaths have occurred (Water Sanitation and Health, 2001). This disease is commonly referred to as Blue Baby Syndrome, and infants are more vulnerable than children (older than 12 months) or adults because infants have a high liquid-based diet and the lack the ability to breakdown nitrate

(Beaudet et al., 2014). Therefore, the U.S. EPA has set the maximum contamination level (MCL) of nitrate-nitrogen in drinking water at 10 mg/L to protect public health (USEPA, 2014). Besides causing Blue Baby Syndrome, nitrite that is converted from nitrate in the body can be further converted into a potent cancer causing chemical known as nitrosamine. The nitrite is believed to react with amine-containing substances found in food to form nitrosamine. However, there is still lack of evidence to confirm the direct link between nitrate intake by humans and formation of nitrosamine (NHDES, 2006).

Denitrification is a key process in water treatment to maintain safe drinking water. Recently in Iowa, Des Moines Water Works (DMWW) filed a lawsuit against three Northwest Iowa counties, which were responsible for the consistently high levels of nitrate in both Raccoon River and Des Moines (DSM) River over the past few years. Nitrate levels in Raccoon and DSM rivers reached record levels of 24 mg/L and 17.9 mg/L respectively in 2013, and remained above the MCL (10 mg/L) in 2014. The high levels of nitrate in this drinking water source forced the water treatment plant to operate the nitrate ion exchange system for 74 days at \$900,000 treatment costs (Des Moines Water Works, 2014). This incident has raised the public awareness of high nitrate levels in Iowa's surface water.

2.2 Transport of Nitrate in Tile Drainage

Tile drainage in agriculture was introduced into the United States in the 1800s. It is later expanded throughout the Midwest region, including Illinois, Ohio, Indiana, Minnesota, Iowa and Missouri because of the unsuitability of swampland for normal cultivation (Kalita et al., 2007). The Federal Swamp Land Acts passed in the 1850 further encouraged the development of swampland for agricultural activities (McCorvie and Lant, 1993). Drainage of excess water from

these agricultural lands has allowed them to be some of the most productive croplands in the world (Kalita et al., 2007). Illinois (3,966,000 ha or 28% of total state land area), Indiana (3,273,000 ha or 35%) and Iowa (3,154,000 ha or 22%) have the largest area of drained lands, and followed by Ohio (2,996,000 ha or 28%), Minnesota (2,579,000 ha or 13%), Michigan (2,233,000 ha or 15%), Missouri (1,717,000 or 10%) and Wisconsin (909,000 ha or 6%) (Kalita et al., 2007).

Even though installation of tile drainage has enabled farmlands to be agriculturally productive, there are also unintended environmental consequences, with the primary concern from the water quality perspective being the increased export of soluble pollutants, especially nitrate (Carlson et al., 2013). Nitrate is a highly water-soluble anion and is not sorbed to negatively charged soil particles. Nitrate is mobile and can be readily leached to tile drains with percolating water (Follett, 1995). While Illinois, Indiana and Iowa have the largest area of drained farmlands, they also contributed the largest percentage (10 to 17%) of estimated nitrate export to the Gulf of Mexico (Kalita et al., 2007). The next major contributor is Ohio (5 to 10%), while other Midwestern states contributes less than 5% respectively (Kalita et al., 2007).

Drainage water is collected in a closed system, which also allows easier monitoring of nitrate loss through tile drainage (Carlson et al., 2013). The average concentration in tile drainage may vary greatly depending on many factors such as nitrogen fertilizer application rate and timing, precipitation, soil type, tile spacing, and land use. In a 16-year study (1989-2004) near Gilmore City, IA where nitrate loss through tile drainage was observed in response to different nitrogen fertilizer application rates, the nitrate concentrations vary from 3.9 mg/L to 28.7 mg/L (Lawlor et al., 2008). Randall et al. (1997) measured 4-year (1990-1993) average nitrate concentration of 32.3 mg/L, 22.8 mg/L, and 25.8 mg/L respectively in continuous corn, corn-soybean rotation,

and soybean-corn rotation cropping systems at Lamberton, MN. A study on relationship between nitrate loss and tile spacing that was conducted in Tippecanoe County, IN reported nitrate concentrations of 22.2 mg/L at 10 m spacing, 17.7 mg/L at 20 m spacing, and 24.3 mg/L at 30 m spacing (Hofmann et al., 2004). A recent study carried out in Webster City, IA reported that more than half (56.1%) of the nitrate export from tile drainage occurs during the upper 10% of daily flow, and concluded that water yield in tile drainage is the primary driver of nitrate export (Ikenberry et al., 2014).

2.3 Denitrification Woodchip Bioreactors

Woodchip bioreactors are an edge-of field denitrification system for treating agricultural tile drainage. They are a subsurface trench filled with woodchips and natural denitrifying microorganisms found in the woodchips or from upland agricultural soils. In most studies, heterotrophic microbial denitrification is recognized as the primary driver for nitrate removal in woodchip bioreactors. These facultative denitrifying bacteria obtain energy by oxidizing organic compounds, and then reduces oxygen and nitrate, although oxygen is more favorable as an electron acceptor (Schipper et al., 2010). Therefore, the woodchip bioreactor is designed to create an anaerobic environment which is desirable for nitrate to be reduced into free nitrogen gas. Other potential removal mechanisms are nitrogen immobilization into organic matter and dissimilatory nitrate reduction to ammonium (DNRA). However, these two mechanism contributed to less than 4% of the nitrate removed (Greenan et al., 2006).

The bioreactor removes nitrate from tile drainage by intercepting and treating a fraction or all of the tile drainage before it is discharged to surface water (Christianson and Helmers, 2011). In a performance evaluation study of four bioreactors in Iowa, Christianson et al. (2012) observed

three of the bioreactors have mean nitrate load reduction of 42% to 75%. Meanwhile, the last bioreactor at Northeast Research and Demonstration Farm (NERF) only has 13% mean nitrate load reduction. Research also has shown bioreactor potential in removing other pollutants such as pesticides, herbicides, antibiotics and phosphorus (Ilhan et al., 2012; Ranaivoson et al., 2012).

On the other hand, studies continue to explore the potential negative impacts of bioreactors such as carbon loading to surface water and greenhouse gas emissions (Christianson and Helmers, 2011; Ranaivoson et al., 2012). During the initial flush of a newly installed bioreactor, a significant amount of Total Organic Carbon (TOC) is observed in the effluent (Gibert et al., 2008). This is unfavorable because high TOC levels in streams may result in higher dissolved oxygen (DO) consumption by microorganisms, creating an unsuitable, low DO level environment for some aquatic species. In a column-scale bioreactor study with 12-hour HRT, Hoover et al. (2015) reported effluent TOC concentration of 222 mg/L at start up, then decreased exponentially to approximately 20 mg/L after 60 days. In a field-scale bioreactor study with 2-8 hour HRT, Bell and Cooke (2015) measured initial effluent Dissolved Organic Carbon (DOC) concentration of 80 mg/L. After 5 months, the DOC concentrations fell below 10 mg/L, which is similar to typical values of DOC in tile drainage that may vary from below 0.3 to 20 mg/L (Ruark et al., 2009). There are also concerns about nitrous oxide emissions, a greenhouse gas (GHG) produced during incomplete denitrification. Greenan et al. (2009) reported that average nitrous oxide production from column bioreactor only accounted for 0.009% of the nitrate added, suggesting that the primary end product was nitrogen gas. In a 9 year field scale study, Moorman et al. (2010) also concluded that the presence of bioreactor in tile drainage did not increase the nitrous oxide emission from tile drainage.

Carbon availability for denitrifiers plays an important role in bioreactor performance. This carbon availability can be impacted by type of carbon substrates and bioreactor HRT (Christianson et al., 2012; Warneke et al., 2011a). Using TOC as indicator for available carbon, Gibert et al. (2008) observed 1.41 milligrams of leachable carbon per gram of hardwood commonly used in bioreactor, which has the second highest TOC concentrations after willow. Christianson et al. (2012) observed higher nitrate removal efficiency in subsequent events after low-flow periods, suggesting that long HRT may have resulted in greater availability of carbon.

Good longevity of the supply of available carbon from the carbon substrate is also important to avoid frequent replenishment. In a five-year study of a mixed-carbon sawdust bioreactor, Schipper and Vojvodic-Vukovic (2001) observed a reduction in available carbon in the first 200 days but stayed relatively constant for the remaining study period. Until today, there are no studied bioreactors that have failed due to carbon exhaustion (Schipper et al., 2010). Although the bioreactor did not fail, it is important to recognize the potential slight decline in nitrate removal rates as available carbon decreases. In 14-year old bioreactors, Long et al. (2011) found that denitrification rates remained high as it was first installed, although the total carbon content was reduced by half. In another similar study, denitrification rates using woodchips from 15-year old bioreactor were 50% of rates measured in the first year (Robertson et al., 2008). A study where comparison were made on 2 and 7 years old woodchips, it was found that both nitrate removal rates remained between 50 to 75% of rates measured in fresh woodchips (Schipper et al., 2010). Moorman et al. (2010) observed 25% and 85% of the carbon remained in unsaturated and saturated interface of bioreactor respectively after 9 years, suggesting that the saturated interface is responsible for continuous nitrate removal in older bioreactors. These studies have

shown that nitrate removal efficiencies remained above 50% after minimum of 7 years, which also evaluated the bioreactor longevity.

2.4 Denitrification Process and Factors Affecting Denitrification Rates

Microbial reduction of nitrate (denitrification) is the primary nitrate removal mechanism that can be found in the natural soil system (IPNI, 2016). This process is carried out by groups of heterotrophic facultative anaerobes, and has the advantage of lower cost and environmental footprint than conventional treatments for removal of nitrate. For the above reasons, denitrification became an attractive and practical approach to remove nitrate through engineered systems such as woodchips bioreactors, drinking water treatment plants and wastewater treatment plants. There are four basic conditions that are required for denitrification to occur. They include active community of denitrifying bacteria, anoxic or anaerobic condition, labile carbon source as electron donor, and presence of nitrate which acts as the electron acceptor.

Denitrification is a multi-step process and each process is governed by multiple different species of denitrifying bacteria, which are also referred as denitrifiers. Initially, nitrate is reduced to nitrite by nitrate reductase (*nar*), and nitrite is further reduced to nitric oxide by nitrite reductase (*nir*). Nitric oxide is then converted into nitrous oxide by nitric oxide reductase (*nor*). Finally, nitrous oxide is reduced to nitrogen gas by nitrous oxide reductase (*noz*) (Hoover, 2012; Zumft, 1997). However, complete denitrification is not always guaranteed to occur, and the quantity of final and intermediate products of denitrification can be highly dependent on environment conditions and other denitrification factors discussed in this chapter. Ultimately, these factors control the gene regulations of the denitrifier, and thus the reaction rates of each intermediate processes. Consequently, the rates of these processes can be estimated by measuring the density

of denitrifying enzymes or quantity of intermediate products (Mania et al., 2016). It is also important to note that denitrifiers represent a wide range of denitrifying genera, some of the common genomes among denitrifying genera include *Bradyrhizobium japonicum*, *Neisseria gonorrhoeae*, *Pseudomonas lemoignei*, *Pseudomonas glathei*, *P. aeruginosa* PAO, *P. aeruginosa* C and *P. fluorescens* (Zumft, 1997). While *Pseudomonas* is the most common and widely distributed denitrifying genus, the complexity and variability of the denitrifier community makes direct quantification of its population difficult. As a result, quantifying the density of functional genes is used as an alternative to estimate the potential of denitrification. In an evaluation of denitrification rates in a system, it is also important to consider other competing pathways of nitrate conversion such as dissimilatory nitrate reduction to ammonium (DNRA). Therefore, it is important to have high diversity of denitrifiers, and thus high functional redundancy for denitrification to stay as the dominant nitrate conversion pathway.

One of the key factors that can affect the denitrification rate is the level of dissolved oxygen (DO) in the water (Gomez et al., 2001). Denitrification is an anoxic process and it requires DO level less than 2 mg/L for denitrification to take place (Hoover, 2012). This is because oxygen releases a higher amount of free energy than nitrate when the molecule is reduced within a cell, and thus making oxygen the preferred terminal electron acceptor (Snoeyink, 1980). In general, the denitrification rate is expected to increase with decreasing DO concentration, provided other parameters are held constant. In woodchip bioreactor, denitrification may occur in the anaerobic microsites of woodchips when DO level is higher than 2 mg/L, although at a lower efficiency (Hoover, 2012). Gomez et al. (2001) observed reduced growth of biofilm in a submerged filter when oxygen is present in excess, as lower denitrifier density is found in the biofilm.

There are mixed results on the effect of varying influent nitrate concentrations on denitrification kinetics in woodchips bioreactors. Ghane et al. (2014) has suggested that first-order rate law provided a better fit than zero-order in the concentration profiles. In contrast, another study conducted by Robertson (2010) showed that nitrate removal rate was insensitive to the change in influent nitrate concentrations, and thus followed a zero-order rather than first-order reaction. At the same time, other studies have shown that nitrate removal rate does not follow either the zero- or first-order reaction rate law. Michaelis-Menten kinetic model is more appropriate in estimating the nitrate removal rate (Ghane et al., 2014; Hoover et al., 2015). In this model, Michaelis constant and maximum reaction rate are used to account for the availability of substrate needed for enzymatic reactions. Nevertheless, these two parameters may vary greatly in different systems, and are subjected to change with changing environmental conditions such as temperature and pH. Hoover et al. (2015) and Ghane et al. (2014) also observed smaller increments in nitrate removal rates when influent nitrate concentration approached 50 mg/L of $\text{NO}_3\text{-N}$, and suggested that nitrate saturation occurs at an approximate range of 30 to 50 mg/L of $\text{NO}_3\text{-N}$. In woodchips bioreactors, the nitrate saturation point can be dependent on the denitrifier density or carbon availability.

The carbon source is one of the major nutrients required for microbial metabolism, as it acts as an electron donor to the microorganism. Studies have reported the influence of the type and concentration of carbon source on denitrification efficiency (Hoover et al., 2015; Mateju, 1992; Robertson et al., 2008; Tan et al., 2013). Mateju (1992) employed stoichiometric equations to determine the required carbon to nitrogen (C:N) ratios for nitrate and nitrite removal. The authors estimated C:N ratio requirement of 1.50, 1.72 and 2.15 using methanol, ethanol, and acetate respectively. In a study using a biofilm reactor which glucose was fed as the carbon

source, Tan et al. (2013) observed that denitrification efficiency increased from 55% to 79% when C:N ratio was increased from 1.8 to 10.5, and proposed that higher organic load improves denitrification. However, Robertson et al. (2008) work has shown that high ratio of organic carbon (alfalfa) to nitrate may favor dissimilatory nitrate reduction to ammonium (DNRA) rather than denitrification. In woodchips bioreactors, the cellulose and lignin compounds in woodchips (inert carbon) are slowly degraded, thus allowing the system to continuously supply labile carbon to the denitrifier over a longer period (Robertson et al., 2008). The statement is supported by other studies on woodchips bioreactors, where high Dissolved Organic Carbon (DOC) levels were observed during the first two to five months start-up period, then decreased to relatively low and constant levels (Bell and Cooke, 2015; Hoover et al., 2015). The rate and concentration of labile carbon released from inert carbon also determine the lifespan of woodchips bioreactor. This is because when the concentration of labile carbon decreases, the denitrifier population decreased correspondingly (Long et al., 2011). Feyereisen et al. (2016) tested corn cob, corn stover, and wheat straw as alternative carbon sources for woodchips bioreactors, and these carbon sources showed greater nitrate removal rates than woodchip. This indicates greater release of labile carbon source into the water, but these carbon sources have the disadvantage in term of longevity, as they are expected to have a shorter lifespan than woodchips. It is also important to recognize that larger amount of carbon source is needed for denitrification when DO level is high (Mateju, 1992). Instead of using carbon as an electron donor, research also has shown the capability of denitrifiers to acquire electrons from H₂ produced through electrolysis of water in biofilm-electrode reactor (BER) (Jing et al., 2015; Prosnansky et al., 2002; Thrash and Coates, 2008). Direct utilization of electrons from the cathodes also has been demonstrated by *Geobacter* species (Thrash and Coates, 2008). Therefore, the integration of woodchips bioreactor

and BER technology may improve the denitrification efficiency by providing multiple sources of electron donors.

In the soil environment, the pH is referred as the “master variable” because of its influence on physical, chemical, biochemical and biological processes. As expected, pH has a large impact on the efficiency of denitrification in woodchips bioreactors. Once again, denitrification is a multi-step biological process, and pH can affect the regulation of each reductase gene that encodes for enzymes required for each denitrification step. Wang et al. (1995) stated that the optimal pH for nitrate and nitrite reduction using *Pseudomonas denitrificans* at 30°C occurs within a range from 7.4 to 7.6, and from 7.2 to 7.3, respectively. They also observed that optimal pH does not vary with nitrate and nitrite concentrations. Furthermore, slight acidic condition (pH<7) is known to inhibit intermediate processes such as the reduction of nitrous and nitric oxide, resulting in the release of those greenhouse gases (Simek and Cooper, 2002). Painter (1970) described that pH should remain above 7.3 to prevent the accumulation of these intermediate products. Saleh-Lakha et al. (2009) studied the effect of pH on denitrification gene expression in *Pseudomonas mandelii*, and reported that quantity of nitrite reductase (*nirS*) and nitric oxide reductase (*cnorB*) genes were 539-fold and 6190-fold lower at pH 5 than at pH 6,7 and 8. The levels of expression of these two genes remain relatively constant from pH 6 to 8, which suggest the stable pH range for nitrite and nitrous oxide reduction. In another study of the long-term effect of low soil pH on natural denitrification rate, Parkin et al. (1985) observed only two-fold decrease in denitrification rates. This suggests the adaptation or selection of acid-tolerant denitrifier population in the natural system. In a nutshell, the optimal pH for a denitrification system may vary based on the type of culture, type of medium, pre-adaptation in buffered solution, and other denitrification factors defined in this chapter. For these reasons, Simek and Cooper (2002) stated that there is

little or no meaning for “optimal” pH, and therefore the skeptical optimal pH range (pH 7-8) should only be used as a guideline and not as a definite optimal pH.

Temperature also has significant impact on denitrification rate. Although denitrifying psychrophilic (-15 to 10°C), mesophilic (20 to 40°C) and thermophilic (45 to 122°C) denitrifiers can be found in the environment, the population is often dominated by the mesophiles (Casella and Payne, 1996). Saleh-Lakha et al. (2009) observed 17-fold and 94-fold increase in *nirS* and *cnorB* gene expression of *Pseudomonas mandelii* after growing at 20°C and 30°C, respectively. In two different studies, denitrification rates of woodchip bioreactors and permeable reactive barrier were observed at the range from 6° to 22°C (Hoover et al., 2015; Robertson et al., 2008). Both the studies reported an exponential increase in nitrate removal rates with increasing temperature.

Although hydraulic retention time does not significantly affect the nitrate removal rate, it is a key factor in designing denitrification systems. Given a relatively constant removal rate, the retention time should be sufficiently long to completely remove the nitrates in the water. However, this may not be practical in a continuous-flow woodchip bioreactor. Therefore, selecting an appropriate hydraulic retention time (HRT) is critical in maximizing the denitrification efficiency of the system. Hoover et al. (2015) observed a positive linear relationship between nitrate percent removal and HRT, when the HRT was increased from 2 to 20 hours. However, total nitrate load reduction decreases statistically with increasing HRT, indicating the decrease in nitrate removal rates when substrate concentration decreases. As a result, HRT of 6 to 8 hours was often selected as the “balanced” operating parameter of woodchips bioreactors, in order to reduce nitrate concentration to EPA drinking water standard (< 10 mg/L) without sacrificing the nitrate removal rate immoderately.

2.5 Bio-electrochemical Reactors for Denitrification

The first reported electrical stimulation of a microbial community to remove toxic pollutants in water dates back to the 1950s (Thrash and Coates, 2008). More recently, the potential of nitrate reduction by stimulating denitrifiers in the presence of carbon source also has been explored (Flora et al., 1994; Sakakibara and Kuroda, 1993). With increasing concern of chemical residual from chemical treatment processes, electrical stimulation became attractive because no chemical amendment is necessary. In addition, bio-electrochemical treatment has the advantage of flexible treatment by culturing diverse species of microorganisms in the reactor. Depending on the treatment objective, oxidizing or reducing zones can be developed using anodes and cathodes respectively. The formation of low oxidation-reduction potential (ORP) zones is favorable for the growth and immobilization of facultative anaerobes, including denitrifying microorganisms, near the cathodes (Sakakibara and Nakayama, 2001). Treatment of contaminants such as uranium, nitrate, ammonia, ferric iron, and other heavy metals have also previously achieved using bio-electrochemical reactors (BER) (Thrash and Coates, 2008; Watanabe et al., 2004). Similarly, the denitrification rate in woodchip bioreactors may be promoted when they are stimulated with electricity. This may be beneficial during spring when the performance of woodchip bioreactors is low, while there is a need to treat larger volume and colder tile drainage. At colder temperature, microbial activity is typically lower but the population remains the same (Feyereisen et al., 2016). By providing alternate readily available energy source from electrical stimulation, the microbial activity and denitrification rate may be temporarily enhanced during spring or other high flow conditions.

In the BER, electrons can be supplied to microorganisms in three potential pathways as illustrated in Figure 2.1. These pathways can then be broken down into two categories: direct

electron transfer and indirect electron transfer (Thrash and Coates, 2008). Direct electron transfer involves the direct interaction of electron transport chain in microbial metabolism and the working electrode, while indirect electron transfer requires a mediator to transfer the electrons from cathode to microorganism. The capability of direct electron transfer has been demonstrated by pure cultures of *Geobacter sp.* in a denitrifying BER that utilized graphite as the working electrode (Gregory et al., 2004). Park et al. (2005) and Wrighton et al. (2010) also have documented the denitrification capability by mixed-cultures consisting of denitrifying microorganisms enriched from wastewater sludge. This projected the potential of using mixed culture in a complex bioreactor, which has greater functional redundancy and stability to degrade nitrates through direct electron transfer. The indirect electron transfer pathways are through electron shuttling and electrolysis of water. In electron shuttling, the electron shuttlers acquire electrons from the working electrode, then donate them to the microorganisms (Lovley et al., 1996; Lovley et al., 1999; Thrash et al., 2007). These electron shuttlers, for examples, quinones, phenazine, and humic substances, are electroactive substrates that can transfer electrons without being degraded (Thrash and Coates, 2008). During electrolysis of water, O₂ and H₂ gas produced at the anode and cathode, respectively, may act as the mediator in the electron transfer process. Alternatively, CO₂ instead of O₂ is produced when a carbon anode is used, which can help to regulate the pH in the water (Sakakibara and Kuroda, 1993; Thrash and Coates, 2008). While internally-produced H₂ can promote denitrification, its overproduction also has shown inhibitory effects on the microbial activity (Thrash and Coates, 2008). Generally, electrolysis of water is considered to be the dominant electron transfer mechanism, and many reactor configurations and operational parameters have been employed to leverage this mechanism (Gregory et al., 2004; Hao et al., 2013; Park et al., 2005; Prosnansky et al., 2002; Thrash and Coates, 2008). In

contrast, Park et al. (2005) and Wrighton et al. (2010) reported that H_2 production from their BER was at least 100-fold slower than the electron uptake rate by the microorganism, thus suspected that direct electron transfer from working electrode was the dominant mechanism. In contrast to the reduction mechanisms above that utilize microorganism, nitrate also may be oxidized or reduced to other nitrogen products by changing the oxidation state of nitrogen through electrochemical reduction. However, this mechanism is unlikely to be significant at low applied potential (Li et al., 2009).

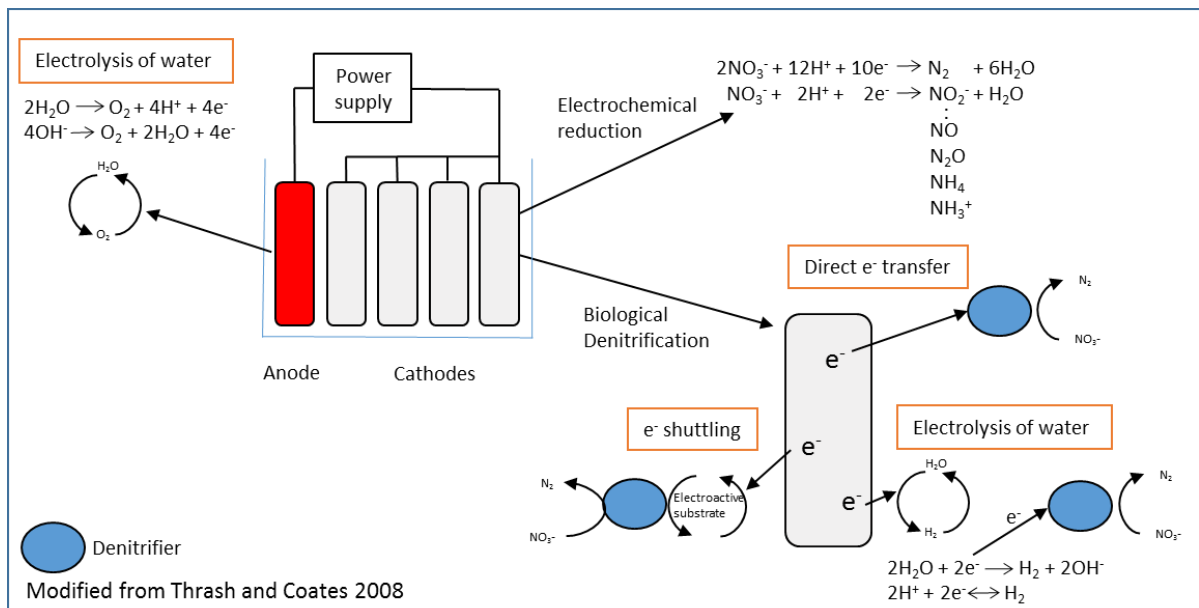


Figure 2-1: Summary of potential electron transfer mechanisms for denitrification in a Bio-electrochemical reactor.

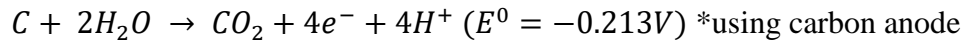
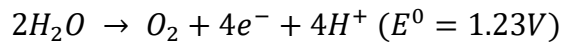
One of the primary factors that could affect the effectiveness of a BER system is the applied potential (Thrash and Coates, 2008). The most common parameters used to control this factor include current intensity and current density. The current intensity has been tested as high as 960 mA, but the usual operating range was found to be between 10 and 100 mA in laboratory scale (Thrash and Coates, 2008). Alternatively, the current density is a measure of current intensity per unit area of cathodic surface. Since cathodic surface area also plays an important role in controlling the performance of a BER, the current density is considered a more comprehensive

control parameter than current intensity. In general, the tested current density ranged from 0.01 to 25 mA/cm², while the optimum current density varied depending on other reactor configurations as discussed below (Prosnansky et al., 2005; Thrash and Coates, 2008). Although higher current density often improves the denitrification rate, a decreased in current-denitrification efficiency was observed at the same time (Prosnansky et al., 2005). In a comparative study, the reactor that did not receive CO₂ buffer exhibited lower denitrification rate at current density higher than 4.67 A/m². This indicated the negative impact of abiotic reaction at electrode surface on microbial activity when operated with higher current density. This is also an important design element to be considered in woodchip bioreactors that have no intrinsic buffering capacity. In addition to the lower cost, low applied potential is desirable to avoid the inhibitory effect from overproduction of H₂ (Thrash and Coates, 2008), and the shift of electric field that may result in unfavorable distribution of nitrate and nitrite molecules (Prosnansky et al., 2005).

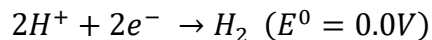
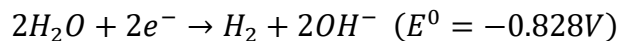
The anode and cathode material also has a significant impact on the BER's performance. In most applications, an inert dimensionally-stable anode, such as titanium, platinum coated titanium and stainless steel, is used as the counter electrode (Li et al., 2009; Park et al., 2005; Sakakibara and Nakayama, 2001; Thrash and Coates, 2008). These noble anode materials which are located at the top of galvanic corrosion chart, are advantageous for their greater durability, thus requires less frequent replacement. Alternatively, graphite or carbon is another commonly used anode in the systems that have no external buffer feeding (Cast and Flora, 1998; Feleke et al., 1998; Thrash and Coates, 2008). As mentioned above, the carbon anode can produce CO₂ when oxidized, which then serves as the pH buffer for the system (Sakakibara and Kuroda, 1993). On the other hand, carbon and stainless steel cathode were also tested for their respective strength.

Besides its lower cost, the carbon cathode has advantage for its irregular and larger surface area, thus promoting greater bacterial adhesion and denitrification rate (Thrash and Coates, 2008). Due to the brittle characteristic of carbon which could impact the maintenance in large-scale treatments, stainless steel cathodes were also experimented, and they showed no statistical difference in denitrification efficiency when compared to the carbon cathodes (Cast and Flora, 1998).

The abiotic reaction in the BER also can result in direct and substantial effect on pH, dissolved oxygen (DO), and oxidation-reduction potential (ORP) around the electrodes (Thrash and Coates, 2008). The following electrochemical reactions can be observed at the anode (Bard and Faulkner, 2001):



and the cathodes:



Besides the applied potential and type of electrode, other BER configurations such as electrode placement and presence/placement of ion exchange membrane, also affect the abiotic reactions and the development of pH, DO and ORP profiles. As shown in the equations above, H^+ ions and O_2 are produced at the anode, thus lowering the pH and increasing the DO level around the anode region. Depending on the anode placement, CO_2 produced from carbon anode may strategically offset the high pH near the cathodes, caused by the production of OH^- ions. Lastly,

oxidizing and reducing zone can be created around the anode and cathode, respectively. Therefore, an appropriate design that takes account of all mentioned interactive factors is required to create an ideal environment with moderate pH, low DO, and low ORP to maximize the denitrification rate. However, there is no single configuration that is commonly recognized as the “ideal” BER’s design. Nevertheless, many previous studies using different reactor configurations have demonstrated successful nitrate removal (Feleke et al., 1998; Gregory et al., 2004; Hao et al., 2013; Li et al., 2009; Prosnansky et al., 2002; Prosnansky et al., 2005; Sakakibara and Kuroda, 1993; Sakakibara and Nakayama, 2001; Thrash and Coates, 2008; Wrighton et al., 2010).

CHAPTER 3 COLUMN SCALE EXPERIMENT

3.1 Theory

Denitrification is a multi-step biological processes accomplished by communities of denitrifiers. These denitrifiers require an electron donor to reduce nitrate to nitrite, and eventually to nitrogen gas. Conventionally, hydrolysis products of woodchips are used as the sole electron donor in woodchip bioreactors. As is typical for biologically mediated reactions, decreasing temperatures results in lower reaction rates (Feyereisen et al., 2016; Hoover et al., 2015). And as is typical for most bioreactor processes that are not mass-transfer limited, lower HRTs are also associated with decreasing nitrogen percent removal in these systems (Hoover et al., 2015). By stimulating the bioreactors with electricity, readily available electrons can be produced to serve as an additional electron donor (Prosnansky, 2002; Thrash and Coates, 2008). As illustrated in Figure 3.1, the electrons can be transferred to the denitrifier from cathodes in three possible ways for biological denitrification: direct electron transfer, indirect electron transfer through electroactive substrates, and indirect electron transfer through hydrolysis of water (Thrash and Coates, 2008).

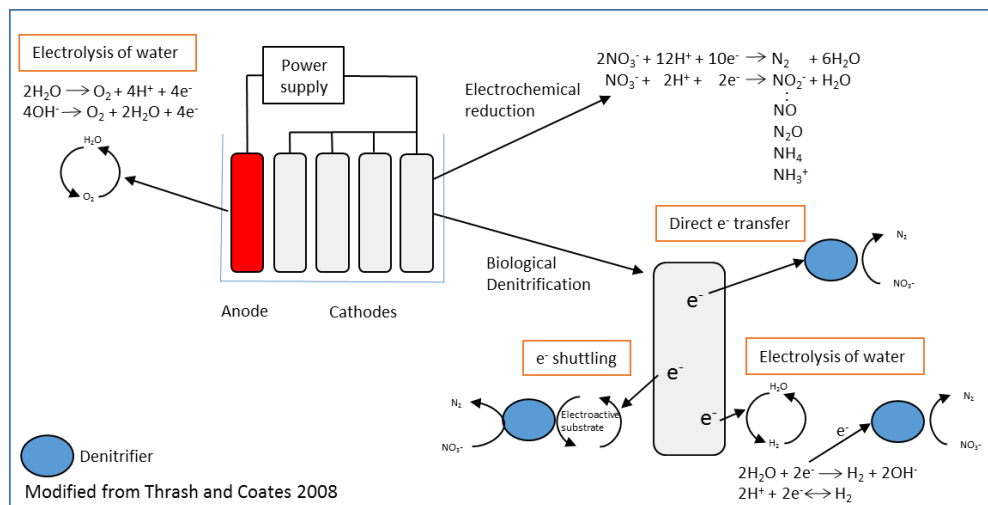


Figure 3-1: Summary of potential electron transfer mechanisms for denitrification in a bio-electrochemical reactor

Direct electron transfer from a graphite cathode to microorganisms to reduce nitrate was demonstrated using pure cultures of *Geobacter* species (Gregory et al., 2004). Furthermore, mixed-culture denitrifying microbial communities enriched from wastewater sludge has been documented to have such capabilities (Park et al., 2005; Wrighton et al., 2010). This suggested the potential of woodchip bioreactors, which employ a diverse microbial consortium (Feyereisen et al., 2016), to remove nitrates through direct electron transfer.

Indirect electron transfer from cathode to microorganism via electroactive substrates is also known as electron shuttling (Thrash and Coates, 2008). Without being degraded, these substrates can accept electrons from the cathode, and then donate to the microorganisms for biodegradation of water pollutants (Lovley et al., 1996; Lovley et al., 1999; Thrash et al., 2007). These substrates include quinones, phenazines, and humic substances (Thrash and Coates, 2008). In theory, humic substances present in woodchip bioreactors could act as electron shuttles, thus improving overall electron transfer efficiency. However, this mechanism has not been studied and its significance is unclear.

Electrolysis of water is another indirect electron transfer mechanism, and different reactor configurations and operational parameters have been employed to leverage this mechanism (Gregory et al., 2004; Hao et al., 2013; Park et al., 2005; Prosnansky et al., 2005; Prosnansky, 2002; Sakakibara and Kuroda, 1993; Thrash and Coates, 2008; Wrighton et al., 2010). In this case, H_2 produced from electrolysis of water can serve as an electron donor for the denitrifying microorganism. However, overproduction of H_2 may result in inhibitory effects (Flora et al., 1994). In some nitrate-removal BERs, ion exchange membrane or sponge was used to keep O_2 , produced at the anode, from entering the cathode region (or nitrate reduction zone), while allowing a passage for proton and electron movement (Prosnansky et al., 2002; Prosnansky et al.,

2005; Sakakibara and Kuroda, 1993; Wrighton et al., 2010). This electrolysis mechanism should be viable in a woodchip bioreactor, although the impact of H₂ and O₂ on the woodchips is uncertain.

Lastly, electrochemical reduction is a non-biological nitrate removal mechanism that may occur in a BER (Li et al., 2009). This mechanism involves the change in oxidation state of nitrogen from nitrate to nitrite, nitric oxide, nitrous oxide, and eventually to nitrogen gas. However, this pathway is not assured, and may result in the formation of by-products that are more toxic (Katsounaros et al., 2012). In addition, it is difficult to achieve selective reduction of nitrate in tile drainage due to the presence of other ions. Nevertheless, it is important to recognize this potential reduction mechanism in a BER, but the reactor configuration in this experiment will be optimized based on microbial reduction pathway.

3.2 Material and Methods

3.2.1 Overview

The experiment had two major phases: An experimental phase examining the performance of electrically-stimulated BERs compared to their non-stimulated controls, and a techno-economic phase where the results from the experimental phase were used to inform a simple spreadsheet-based model of full-scale BER cost.

3.2.2 Experimental phase – reactor overview

The experiment was designed to compare the nitrate removal efficiencies with and without electrical stimulation. Furthermore, different anode materials were evaluated in duplicate, 316-

stainless steel (SS) and graphite (C). Graphite was used as cathodes for all columns. During the start-up period, all columns were flushed with nutrient solution for 31 days to remove excessive Total Organic Carbon (TOC), and to inoculate denitrifying bacteria. Two pairs of BERs with 100 mA applied current and a pair of control reactors were then tested under 10°C for 39 days, but no nitrate removal (data not shown) was observed in all BERs and control reactors. The same finding was reported by Feyereisen et al. (2016) in woodchip bioreactors. The data of 100 mA electrical treatments at 10°C was not discussed in the following sections because we did not even observe an improvement of the same electrical treatments at room temperature. Therefore, we can expect the same explanation from room temperature to be applied on 10°C scenario, in addition to the explanation where minimal microbial activities can be expected at low temperature condition. Consequently, the operating temperature was increased to room temperature (22.5°C), and re-inoculated with denitrifying bacteria during an 11-day transition period. Then, the effect of current intensity on nitrate removal was evaluated by supplying 500 mA and 100 mA to the BERs in two consecutive periods. Difference in denitrification efficiency between BERs and control reactors was observed during the room temperature study. As a result, here we report only the effect of electrical stimulation under room temperature conditions (Condition B and C). The test summary of this experiment is presented in Table 3.1.

Table 3-1: Summary of operating conditions including current intensity, temperature and hydraulic retention time (HRT) in three respective testing periods. HRT can be obtained by dividing pore volume with flow rate.

Condition	Day	Number of day	Current (mA)	Temp (°C)	HRT (hr)
Start-up period	0 - 31	31	0	10	5.9
A	32 - 70	39	100	10	5.9
Transition period	71 - 81	11	100	22.5	8.2
B	82 - 128	47	500	22.5	8.2
C	129 - 149	21	100	22.5	8.2

3.2.3 Reactor vessel and packing

The experiment was conducted with three pairs of duplicated up-flow column woodchip bioreactors. Each chamber measured 15.2 cm (6 inches) in diameter and 50.8 cm (20 inches) in height. A pair of diffuser plates and a pair of flexible caps were fit onto each end chamber. One anode socket and two cathode sockets, which consisted of 2.5 cm (1 inch) diameter electrode, 3.8 cm diameter (1.5 inches) PVC slot, and 3.8 cm diameter (1.5 inches) flexible cap, were inserted into the sides of the chamber as shown in Figure 3.2. The electrodes were 101.6 cm (40 inches) long. The chamber, sockets, and diffuser plates were made of polyvinyl chloride (PVC).

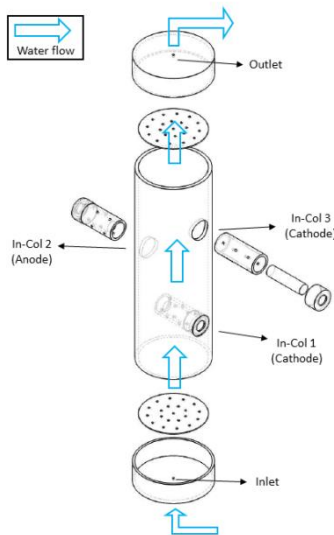


Figure 3-2: Exploded view of up-flow bio-electrochemical reactors. Blue arrow represents direction of water flow, which flows from inlet (bottom) to outlet (top) of the reactors. In-Col 1 and 3 are the locations of cathode; In-Col 2 is the location of anode.

Each reactor with total volume of 9.47 L was packed with 2 kg of hardwood chips (Golden Valley Hardscapes, Story City, Iowa), resulting in a mean pore volume of 4.91 ± 0.1 L (mean \pm SD). The average gravitational and internal porosity of the woodchip media were 0.52 ± 0.01 and 0.32 ± 0.03 , respectively. This yield a total porosity of 0.84, which was comparable to 0.84 and 0.89 reported by Robertson (2010) and Hoover et al. (2015), respectively.

3.2.4 Electrical stimulation system

SS-C (anode-cathode) electrode combinations were employed in a pair of duplicated columns, while C-C electrode combinations were tested in the second pair of duplicated columns. The last pair of duplicated columns without electrodes (and power supply) was served as controls.

The anode was placed in the center of the chamber, which was also located between the two cathodes (Figure 3.2). The anode measured a distance of 25.4 cm (10 inches) from both inlet and outlet. Meanwhile, each cathode was 12.7 cm (5 inches) apart from anode, and inlet or outlet. All electrodes were connected to the power supply (Labnet Enduro™ E0303).

The BERs receive no electrical stimulation during the start-up period, and were supplied with 100 mA (7.52 A/m^2) current during the 10°C testing period (Table 3.1). During the 11-day transition period for the temperature adjustment, 100 mA of current was supplied to the BERs. Then, the BERs received current intensity at 500 mA (37.6 A/m^2) for 47 days, and finally 100 mA for the last 21 days of operation.

3.2.5 Fluid handling system

Two 4-channel variable speed peristaltic pumps (Ismatec CP 78017-10) were used to supply nutrient solution to all columns. Flow rate setting was tuned and appropriate tubing size was selected to achieve average HRTs of 5.9 and 8.2 hours (Table 3.1). The HRTs were estimated using measured pore volumes. Flow rates of the pumps were occasionally adjusted based on measured daily average flow rate, to compensate the variations due to tubing wear and other factors. Tubing was replaced when flow rate decreased significantly. Synthetic nutrient solution containing 30 mg/L of $\text{NO}_3\text{-N}$, and other micronutrients (detailed in supplementary information) required for optimal bacterial growth (Nadelhoffer, 1990), was used to represent tile drain water

(Hoover et al., 2016). The solution was prepared in a 170 L container as influent solution for all columns.

3.2.6 Thermal control

As mentioned above, the columns were initially placed in a temperature-controlled room at 10°C. However, no nitrate removal was observed in our cold temperature study (data not shown), which similar result was also reported by Feyereisen et al. (2016) in their 1.5 and 15.5°C woodchip bioreactors experiments. Therefore, the temperature was increased and maintained at 22.5°C for the rest of the experiment. Due to the local heating effect from electrical stimulation, the temperature was monitored at Inlet, In-Col 1, In-Col 2, In-Col 3 and Outlet (Figure 3.2) on a weekly basis.

3.2.7 Microbial inoculation

One *Klebsiella* (DN2) and two *Raoutella sp.* (DN3 and DN8A) were obtained from Moorman's laboratory culture collection. These bacteria used in the BERs were originally isolated from soil and they were confirmed to be denitrifying bacteria through their ability to produce N₂O from NO₃-N under O₂-free conditions in the presence of acetylene (Tiedje, 1994). They were inoculated into 25 mL of nutrient broth, and incubated at 30°C on a rotary shaker for 4 days. Then, they were harvested by centrifuging at 5000 x g for 20 minutes. Cell pellets of each strain was re-suspended in 25 mL sterile phosphate buffer solution, respectively, and plated to determine cell concentrations before added together to form a 75 mL mixed culture. The first mixed culture was added into a large influent container containing nutrient solution during the

start-up period (Day 19), and fed continuously to each reactor for 24 hours. During Day-2 of the transition period (Day 72), the mixed culture was regrown and added into the influent tank.

3.2.8 Sample collection

Influent and effluent $\text{NO}_3\text{-N}$ samples were collected every other day. Influent $\text{NO}_3\text{-N}$ sample was collected directly from the influent tank; 1-day (3 or 4 pore volumes) composite samples of effluents were collected from respective effluent container. All $\text{NO}_3\text{-N}$ samples were preserved with hydrochloric acid and stored at 4°C until analysis. In addition, instantaneous pH, ORP and DO samples of each reactor were collected weekly at five different locations: Inlet, In-Column 1, In-Column 2, In-Column 3 and Outlet (Figure 3.2). These samples were analyzed immediately. TOC samples were only collected after the color intensity of the effluent was reduced from dark to light tea color at Day-10. Daily samples were collected until Day-18, when average TOC concentration (3.6 ± 0.8 mg/L) was reduced to typical background concentration (< 5 mg/L DOC) observed in Iowa's surface streams (Ruark et al., 2009). TOC samples were preserved with phosphoric acid and stored at 4°C until analysis. At the end of experiment, the reactors were deconstructed and woodchip samples were collected from each reactor for microbial analysis. Woodchip samples were obtained from Inlet, In-Col 1, In-Col 2, In-Col 3 and Outlet. All microbial samples were frozen until DNA extraction and qPCR analysis.

3.2.9 Analytical method

$\text{NO}_3\text{-N} + \text{NO}_2\text{-N}$ concentration was determined using Seal Analytical Method EPA-114A, rev. 7, which is equivalent to U.S. EPA method 353.2. Since there was no nitrate removal observed in all reactors during the 10°C experimental period, the data was excluded and performance of each

reactor was only evaluated under room temperature conditions. In addition, only data with daily influent concentration of 30 ± 4 mg/L was used for data analysis to exclude the effect of influent concentration on nitrate removal efficiency. Denitrification efficiency (DE) was calculated using the following formula:

$$DE = \frac{(C_{NO3-N,inf} - C_{NO3-N,eff})}{C_{NO3-N,inf}} \times 100\%$$

where $C_{NO3-N,inf}$ and $C_{NO3-N,eff}$ are influent and effluent nitrate concentration (mg/L). Statistical analysis was conducted to compare the DE of each treatment and control, using ANOVA (normal distribution) and Wilcoxon test (non-normal distribution) in JMP software. All datasets were tested for normality using QQ-normal plot. P-value ≤ 0.05 was used for all statistical analysis. The current intensity and type of treatment were considered as nominal data, while nitrate removal efficiency was treated as continuous data. In addition, current-denitrification efficiency (η , %) was calculated using the formula below (Prosnansky et al., 2002):

$$\eta (\%) = \frac{Q(C_{NO3-N,inf} - C_{NO3-N,eff})}{I/nF} \times 100\%$$

where Q is volumetric flow rate (cm^3/s), $C_{NO3-N,inf}$ and $C_{NO3-N,eff}$ are influent and effluent nitrate concentration (mol/cm^3), I is current intensity (A), apparent n is stoichiometric coefficient [$n = 5$, representing the change in oxidation number of N from NO_3^- N (+5) to N_2 (0)], and F is Faraday's constant (C/mol).

For TOC analysis, persulfate-ultraviolet oxidation method was employed using Teledyne Tekmar Phoenix 8000 TOC analyzer. This is Method 5310 C in Standard Methods for the Examination of Water and Wastewater, 22nd Ed.

The pH and ORP were measured using Thermo Scientific Orion Star A324, configured with pH (Orion™ ROSS Ultra pH/ATC Triode) and ORP (Orion™ 9678BNWP ORP/Redox electrode) probe, respectively. DO was measured using a DO meter (YSI ProODO™).

The microbial woodchip samples were thawed and chopped to approximately 0.5 cm wide and 1 to 2 cm long. Genomic DNA was isolated from woodchip samples using DNeasy PowerMax Soil Kit (QIAGEN, Inc., Germantown, MD) according to manufacturer's protocol. DNeasy qPCR was targeted for *nosZ* denitrification genes (nitrous oxide reductase). In addition, *16-rDNA* genes were also quantified to obtain total gene number of Eubacteria so that relative abundance of *nosZ* gene can be determined. The detailed methods which were consistent with Kandeler et al. (2006) and Feyereisen et al. (2016) are provided in SI. The relative abundance of *nosZ* gene at the anode (In-Col 2 sampling location) was excluded from column average because of the oxidizing condition which may favors the growth of other microbes.

3.2.10 Preliminary technoeconomic analysis

A preliminary technoeconomic analysis (TEA) was conducted to provide a rough estimate of the cost (in US\$, or USD) to remove a unit mass (kg) of NO₃-N in full-scale reactor. A base case with no electrical stimulation and four BER scenarios were created (Table 3.2). The TEA includes three major costs associated with a BER: capital, operating, and maintenance costs. Capital costs were estimated using traditional woodchip bioreactor construction costs, which includes excavation, structure, and woodchips (Christianson et al., 2013). Cathode costs were also treated as capital costs because they are not expected to degrade and are therefore one-time costs. The BER operating costs were for electricity, which were based upon scaling power per unit volume from the small to full-scale reactors, and upon electricity rates assumed at \$0.08/kWh. However, the BER was expected to operate with electrical stimulation under high-flow conditions only, which was assumed to be 10% annually (Ikenberry et al., 2014). The maintenance costs were for anode replacement, which were based upon anode degradation rates observed in the experimental reactors. It is important to note that this simple TEA did not account for the cost differences that can be caused by actual dimension (width: length: depth ratios) of the reactor, local availability of woodchips, distance of power line to bioreactors, wiring installation, engineering design fee and other detailed factors. Nevertheless, these estimated removal costs would serve as a preliminary work to determine the relative cost difference between electrical treatments and traditional woodchip bioreactors, and also to provide an insight on the strategy for cost reduction.

Table 3-2: Input summary of techno-economic analysis. Interest rate 5%.

	Unit	Base Case	Scenario 1	Scenario 2	Scenario 3	Scenario 4
Cost						
Capital cost	\$/yr	627	1042	1042	1042	1042
Maintenance cost	\$/yr	0	402	1064	1753	1064
Operating Cost	\$/yr	0	441	441	7321	7321
Benefit						
Nitrate mass removal	kg NO ₃ -N/yr	129	136	122	215	150
Other input parameters						
Electrode pair		N/A	C-C	SS-C	C-C	SS-C
Anode: Reactor Volume	m ³ /m ³	N/A	0.024	0.024	0.024	0.024
Anode lifespan	yr	N/A	6.4	15	1.3	15
Cathode: Reactor Volume	m ³ /m ³	N/A	0.047	0.047	0.047	0.047
Current density	A/m ²	N/A	7.52	7.52	37.6	37.6
Nitrate mass removal	%	18.5%	20.4%	16.6%	40.5%	24.0%

For the capital costs, we assumed a full-scale reactor excavation volume of 100 m³. This in turn was used to estimate excavation, structural and woodchip costs (Christianson et al., 2013). The capital costs were amortized assuming 15 years operational life and 5% annual interest. No depreciation, salvage, or tax costs/benefits were assumed. The mass of cathodes required in full-scale treatment was determined based on ratio of cathode mass to reactor volume in the lab-scale experiments.

The anode material was considered as a maintenance cost due to the necessity for replacement over time. It was assumed to have same anode and cathode loading factors (m³/m³) as our lab reactors (Table 2). The anode lifespan was projected based on the anode corrosion rate during the 149-day laboratory experiment. This yielded an estimated graphite anode lifespan of 6.4 years at 7.52 A/m² (or 100 mA in our lab reactor), and 1.3 years at 37.6 A/m² (or 500 mA) operating current. In contrast, the stainless steel anode was projected to have much longer lifespans at 349

and 69.9 years respectively. This effectively meant that the stainless steel anode was a one-time cost for our analysis. No salvage value was considered.

In this analysis, the nitrate removal efficiency of the full-scale BERs was expected to be equal to the results in our laboratory experiment. We also assumed treatment area of 22.2 hectares with nitrate export rate at 31.4 kg NO₃-N/ha-yr (Christianson et al., 2013; Ikenberry et al., 2014). We assumed 56% of the nitrate is during 10% of daily flow, and that this drainage water was treated with electrical stimulation; the remaining 44% would be treated without electrical stimulation (Ikenberry et al., 2014). The nitrate removal efficiency (18.5%) of traditional treatment was assumed to be the same as our control reactors. The nitrate mass removal of each scenario was presented in Table 3.2, and was considered as the “benefit” in this analysis.

Finally, the N removal cost was calculated by taking the ratio of total cost over total benefit (nitrate mass removal). A sensitivity coefficient analysis was performed on key parameters including bioreactor construction cost, cathode cost, incentive program, anode cost, anode lifespan, electricity cost, and nitrate mass removal.

3.3 Results and Discussions

3.3.1 Effect of electrical stimulation on denitrification efficiency

The effect of electrical stimulation on percent denitrification efficiency (DE) or percent nitrate removal efficiency was evaluated by supplying current at 100 mA (Day 82-128) and 500 mA (Day 129-149) to two pairs of BERs (SS-C and C-C), respectively, under room temperature conditions (Figure 3.3). The DEs of electrically stimulated BERs was compared to control reactors, which were not electrically augmented. At 100 mA, the average DEs of SS-C and C-C treatments were $16.6 \pm 4.8\%$ (mean \pm SD) and $20.4 \pm 13.0\%$, respectively. Meanwhile, the control reactors showed an average DE of $18.5 \pm 7.0\%$. Denitrification efficiency of SS-C ($p =$

0.53) and C-C ($p = 0.61$) treatments was not statistically different from the controls; suggesting that denitrification efficiency was not improved using electrical stimulation at 100 mA. Alternatively, SS-C and C-C treatments yield average DEs of $24.5 \pm 11.4\%$ and $41.1 \pm 21.2\%$, respectively, when stimulated with current at 500 mA. The DE of the control reactors during this experimental period was $12.3 \pm 4.2\%$, which was statistically lower than the DEs of SS-C ($p < 0.01$) and C-C ($p < 0.01$) treatments. This demonstrated the enhancement of denitrification efficiency using electrical stimulation at 500 mA. The lack of electrical influence on DE at 100 mA, and improvement on DE observed at 500 mA was because of our low current-denitrification efficiency, which will be detailed in the next section.

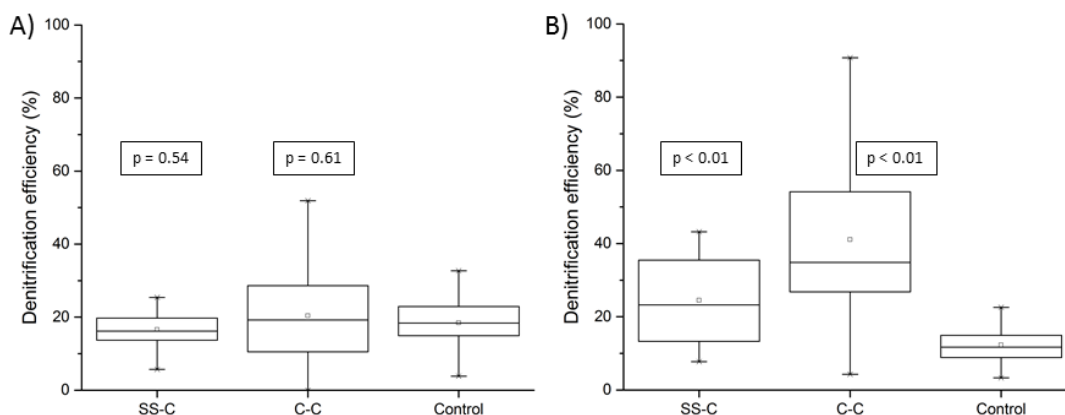


Figure 3-3: Denitrification efficiency of each treatment at 100 mA (A) and 500 mA (B). SS-C: stainless steel anode-carbon cathode; C-C: carbon anode-carbon cathode

3.3.2 Effect of current density on denitrification efficiency and current-denitrification efficiency

DEs were consistently higher at 500 mA than 100 mA in both treatments ($p < 0.01$). Alternatively, the estimated values of current-denitrification efficiency (η) decreased with higher current intensity. The η in this experiment was estimated by assuming all electrons uptaken by denitrifiers for denitrification in electrical columns were obtained from the cathodes, which were also a more readily available electron source. The η of SS-C and C-C treatments at 100 mA

treatments were 28.7 and 35.2%, respectively. Our observed η were lower than Prosnansky et al. (2005)'s optimum η (61.5%), which was likely due to smaller cathode surface area in our reactors, as compared to the volume of our BERs. However, this comparison should only be used as a reference and no direct comparison should be made due to the other differences in the reactor design and type of carbon source used. With small η and lower current intensity in our BERs, fewer electrons were provided to the denitrifiers at 100 mA. Accordingly, DEs were improved when the BERs received five times more electrons when current was supplied at 500 mA. This observation suggested that DE can be improved by supplying sufficient electrons using higher current intensity, although it is important to note that the η (SS-C: 9.4 %; C-C: 14.2 %) at 500 mA was further reduced. In other words, more electrons were delivered to denitrifiers for denitrification, but even more electrons were not utilized by the denitrifiers. One of the possible reasons was because larger fraction of electrons was lost due to excessive production of H_2 gas, which was not utilized by the denitrifier (Figure 3.1). This trend was consistent with Prosnansky et al. (2005)'s comparative study where decreased in η was observed with increasing current intensity. It also became less economically feasible when the required current intensity or current density for the BERs increases.

Moreover, the maximum denitrification potential was not achieved in our reactors. The DE and η can be improved by increasing the cathode surface area, while maintaining low current density. Higher DE and η reported by Prosnansky et al. (2005) was likely due to their larger cathode surface area per unit pore volume (m^2/m^3). Prosnansky et al. (2005) had a reactor which used 123 m^2 of graphite cathodes per cubic meters pore volume, while our reactor's graphite cathode loading factor was only 15 m^2/m^3 . Since cathode surface area plays an important role in electron transfer efficiency, appropriate current density (current intensity/cathode surface area) is

recommended to be used to select the suitable current intensity when rescaling the BER for full-scale practices. Other reactor configurations such as placement of electrodes and use of ion exchange membrane also can be modified for better denitrification efficiency and η , which will be discussed in the last section of this paper.

3.3.3 Effect of anode material on denitrification efficiency

No significant difference in DE was found between SS-C and C-C treatments at 100 mA ($p = 0.33$). However, there was a significant difference in DE between the two treatments at 500 mA ($p < 0.01$). The C-C treatment (41.1 ± 21.2 %) demonstrated the highest average DE, followed by the SS-C treatment (24.5 ± 11.4 %) and control reactors (12.3 ± 4.2 %).

The higher removal efficiency in C-C treatment was likely due to the oxidation of graphite anode into CO_2 , which provided a buffering capacity for the system (Thrash and Coates, 2008). Despite its higher DE, corrosion of the graphite anode was also significant. An average mass loss of the graphite anode was $65.1 \pm 16.9\%$ after receiving 100 mA current for 71 days, and 500 mA current for 47 days. In contrast, O_2 was produced at the anode of SS-C treatment, causing the DO level at locations above the anode (In-Col 2, In-Col 3 and Outlet) to elevate. Higher DO level in SS-C treatment was likely to impact its DE, as observed in this experiment. Only $1.22 \pm 0.3\%$ of the stainless-steel anode in the SS-C treatment was degraded throughout the experimental period. For this reason, N removal cost of using each anode material was evaluated in TEA.

3.3.4 Factors affecting pH, ORP, and DO and their effect on denitrification efficiency

Despite the improved DE observed in BERs, it is important to recognize the high variability in DE of the BERs at 500 mA, which was likely due to the inconsistent pH and ORP profile within the reactors. As presented in Figure 3.4, the pH and ORP values at each sampling location of each BER varied greatly (error bars) even though the current intensity and water flow rate were kept constant during the treatment periods.

At 100 mA, the pH at sampling location In-Col 1 (cathode) in both SS-C and C-C treatments increased due to production of OH^- ions at the cathode. The pH was then decreased at In-Col 2 (anode) as H^+ ions were produced at the anode. Unsurprisingly, the pH at In-Col 3 (cathode) in SS-C treatment was increased. However, pH at In-Col 3 in C-C treatment remained at approximately 6.3 (Table S2). It was suspected that CO_2 produced at the anode of C-C treatment act as a pH buffer for the upper half of the column. At 500 mA, pH profile in all BERs shared the same trend: increased at In-Col 1, then decreased along the reactor, and finally leveled off around 5.73 at In-Col 3. The pH pattern at In-Col 1 and In-Col 2 followed the same explanation for 100 mA scenario. Interestingly, the pH at In-Col 3 did not increase even in the SS-C treatment. This was likely due to better mixing of H^+ and OH^- ions in the upper half of the reactor resulted from greater production of gas bubbles at higher current intensity. Nevertheless, the greater swing of pH in SS-C treatment possibly contributed to its lower nitrate removal efficiency as compared to the C-C treatment.

Lower ORP values were observed in electrical treatments than in controls (Figure 3.4), which indicated a better reducing condition for denitrification. Recall that reducing zone is formed around the cathode, while oxidizing zone is created around the anode. As expected, the ORP values at 100 mA scenario decreased after the influent enters BERs at In-Col 1 (cathode), and

then increased at In-Col 2 (anode). Finally, the ORP decreased again as water passed through In-Col 3 (cathode). At 500 mA, even lower ORP values were observed in SS-C treatment but the values remained relatively the same in C-C treatment, as compared to 100 mA scenario. This suggested that a better reducing condition can be created with SS-C treatment, despite the pH (discussed in previous paragraph) and DO (discussed in next paragraph) issues in this up-flow column design. Take note that the ORP profile at 500 mA did not follow the same and obvious trend as observed in the 100 mA scenario, which was also likely due to greater mixing at upstream from gas bubbles produced at downstream.

Meanwhile, average DO of the influent was 7.9 ± 0.3 mg/L, but immediately reduced to an average of 1.6 ± 0.5 mg/L after entering the reactors at In-Col 1 (Figure 3.4). This suggested microbial activity took place immediately by consuming oxygen. In addition, In-Col 1 was located below anode (In-Col 2), thus leaving it unaffected from O_2 or CO_2 produced at the anode. In both 100 and 500 mA scenarios, the DO levels in SS-C treatment increased at the anode (In-Col 2) and upstream of anode (In-Col 3 and Effluent). However, DO levels at all sampling locations in C-C treatment remained below 2 mg/L. This was because O_2 was produced at anode of SS-C treatment, while CO_2 was likely produced at the anode of C-C treatment. Consequently, the higher DO level in the SS-C treatment may explain the lower DE when compared to the C-C treatment, although equal amount of external energy source (electron) was provided.

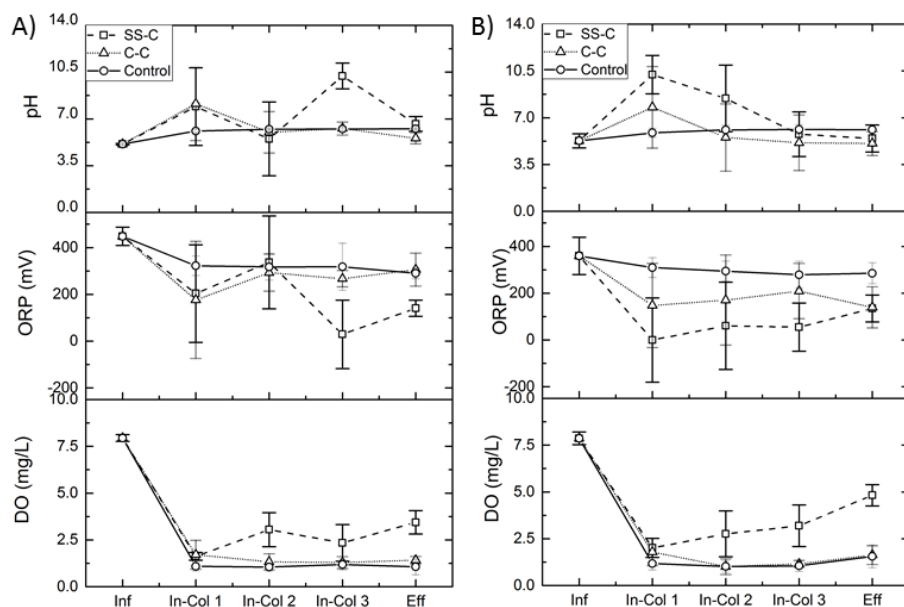


Figure 3-4: pH, ORP and DO of each treatment at 100 mA (A) and 500 mA (B). SS-C: stainless steel anode-carbon cathode (dashed line, widest error bar cap); C-C: carbon anode-carbon cathode (dotted line, medium width 50% transparency error bar cap); control (solid line, narrowest 75% transparency error bar cap).

3.3.5 Denitrifying bacterial communities and their role in denitrification

The abundance of denitrification genes ranged from 2.02×10^{11} to 2.96×10^{12} copies of *nosZ* g^{-1} dry substrate in SS-C treatment; 1.35×10^{10} to 1.56×10^{11} copies of *nosZ* g^{-1} dry substrate in C-C treatment; and 3.05×10^{11} to 3.11×10^{12} copies of *nosZ* g^{-1} dry substrate in control reactors (Table S3). Meanwhile, the abundance of EUB genes ranged from 4.15×10^{12} to 1.70×10^{14} copies of EUB g^{-1} dry substrate in SS-C treatment; 3.10×10^{12} to 2.24×10^{13} copies of EUB g^{-1} dry substrate in C-C treatment; and 3.70×10^{10} to 1.14×10^{11} copies of EUB g^{-1} dry substrate in control. The gene abundances in C-C treatment were lower than the SS-C treatment and control, but all values were comparable to other studies where active denitrifying genes were quantified (Feyereisen et al., 2016; Ilhan et al., 2011; Kandeler et al., 2006; Warneke et al., 2011b). This suggested that microbial denitrification can occur in electrical treatments and the control, with possible electrochemical reduction of nitrate in electrical treatments. However, microbial reduction was likely to be the dominant nitrate removal mechanism because if electrochemical

reduction was the dominant mechanism, then the change in current intensity from 500 to 100 mA is expected to yield a much lower nitrate removal efficiency (~ 4-5 times lower) than what was observed. The notable effect of DO level on DEs between SS-C and C-C treatments at 500 mA further proposed that microbial denitrification was the dominant mechanism; although, the electron transfer pathway (direct vs indirect) cannot be determined from our experiments.

The average relative abundances of *nosZ* gene from two replicated SS-C columns were 1.3% and 0.9%, respectively. In the duplicated C-C columns, the average relative abundances were 0.4% and 0.6%, respectively. Meanwhile, the control reactors had 1.2% and 1.3% relative abundance of *nosZ* gene, respectively. The lower gene abundance and relative abundance in C-C treatment suggested that electrical stimulation may alter the total population and density of microbial communities in the BERs. This may be caused by differences in pH, ORP and DO levels, as well as growth capabilities of denitrifiers and other microbes by utilizing electrons from electrical stimulation. Therefore, it is important to recognize the presence of other microbes, which may outcompete the growth denitrifiers if the environmental conditions become favorable.

3.3.6 Technoeconomic analysis

As presented in Figure 3.5, the electrical treatments or BERs did not appear to be an attractive approach from the perspective of its additional costs with respect to the benefit of improved denitrification efficiency. The base case, which resembles the traditional woodchip bioreactor had nitrate removal cost at \$4.86/kg NO₃-N. Our estimated value was almost four times greater than the estimation (\$1.07/kg NO₃-N) by Christianson et al. (2013). The divergent of our base case as compared to Christianson et al. was due to the differences in several input parameters, which includes lifespan of woodchip bioreactors (15 vs 40 years), interest rate (5 vs 4%), and

denitrification efficiency (18.5 vs 37.5%). Consequently, our BER scenarios were only compared to our base case.

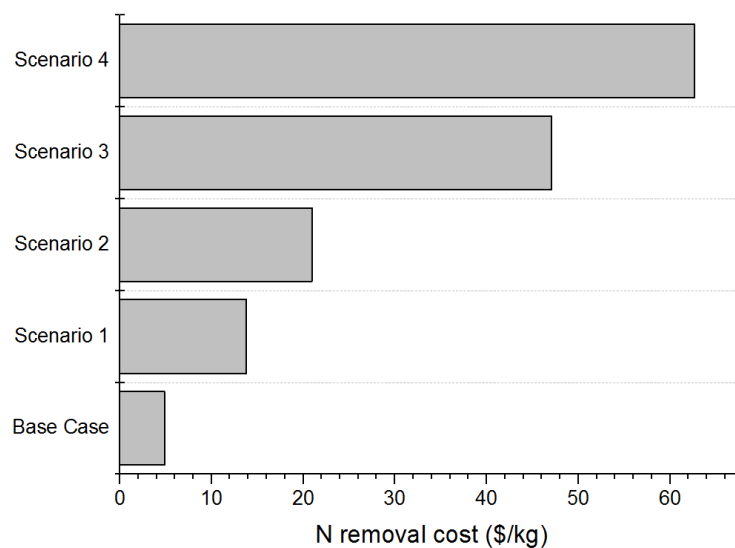


Figure 3-5: Comparison on nitrogen removal costs of using electrical approach for denitrification in woodchip bioreactors.

Scenarios 1 and 2, which corresponded to the low operating current (7.52 A/m^2) had much higher N removal costs compared to base case. Nevertheless, the N removal cost of Scenario 1 can be reduced to base case level with 85% nitrate removal efficiency (data not shown), which can be potentially achieved with a well-designed reactor. The high-current scenarios were even less cost effective. We explored how the cost per unit N removed would change if Scenarios 3 and 4 achieved 100% N removal (data not shown) – but those scenarios were still not economically competitive with the base case.

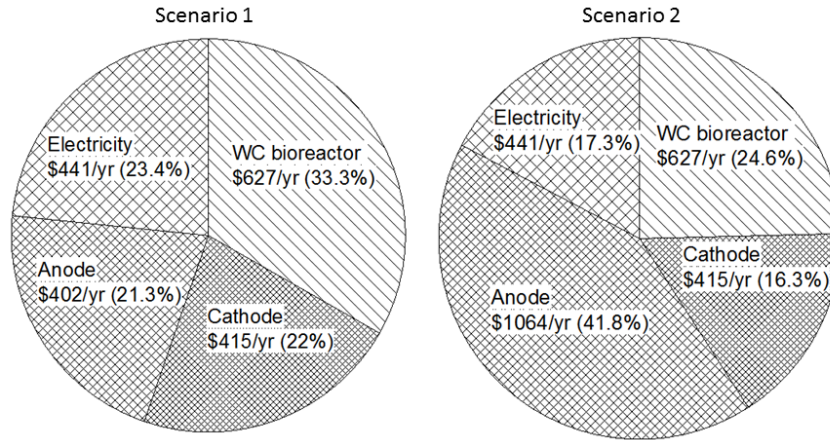


Figure 3-6: Cost breakdown of scenario 1 and 2. Each scenario's assumptions were summarized in *Table 3.2*.

A few of the primary reasons that contributed to the high cost of BER include cathode installation cost, anode maintenance cost and electricity cost. BER typically requires a large cathode surface area, which yield the additional cost with respect to traditional WC bioreactors. In Scenario 1, the high degradation rate of graphite anode resulted in frequent need for replacement every 6.4 years, thus contributed to a large portion of the total cost. Although stainless steel anode (Scenario 2) had a much lower degradation rate and does not require replacement, it had a significantly higher material cost than graphite. The sensitivity coefficient analysis for Scenario 1 found that 1% increment in bioreactor's construction cost, cathode cost, anode cost and electricity cost will increase N removal cost by 0.51%, 0.23%, 0.22% and 0.25%, respectively (Table S4); while the sensitivity coefficient analysis for Scenario 2 shown that bioreactor's construction cost, cathode cost, anode cost and electricity cost will increase N removal cost by 0.45%, 0.20%, 0.32% and 0.22%, respectively. This suggested that better denitrification efficiency (thus lower HRT, smaller reactor size), smaller anode, and lower current intensity can be the key to reduce N removal cost of BER. A better denitrification efficiency can be attained in horizontal-flow reactors as described in Prosnansky et al. (2005). Since SS anode undergo little degradation over a long period, its size can be reduced significantly. Finally, lower current intensity can be used to achieve the same or higher

denitrification efficiency by improving the η in both scenarios. This can be achieved by using cathode shape that would yield a larger surface area given the same mass.

3.4 Conclusion

This study has demonstrated the improvement on nitrate removal efficiency of woodchip bioreactors using electrical stimulation. The primary nitrate removal mechanism of these electrically modified reactors was suspected to be microbial denitrification. Higher denitrification efficiencies using SS-C ($24.0 \pm 11.0\%$) and C-C ($40.5 \pm 19.5\%$) BERs were obtained, as compared to control woodchip bioreactors ($14.0 \pm 6.5\%$). However, the enhanced denitrification efficiency also arose with additional costs associated with material cost of electrodes and electricity cost. In a well-designed BER, the additional costs may be offset with greater denitrification efficiency.

3.5 Implication of Work and Future Research

In this experiment, we found that up-flow woodchip bio-electrochemical reactors were difficult to operate and did not achieve the expected denitrification potential. This is because it was difficult to optimize the three denitrification criteria (pH, ORP, DO) altogether in an up-flow reactor without the use of pH buffer. Recall that ideal zone for denitrification includes somewhat neutral pH, low ORP and low DO. Initially, we aimed to offset the pH difference at anode and cathodes by placing the anode in between the two cathodes. However, inconsistent and extreme pH was still observed in some locations adjacent to electrodes. Due to the center location of anode, distinct oxidizing and reducing zones were not created. The reducing zone, where denitrification takes place, need to be larger and separated from oxidizing zone for better denitrification. In addition, the DO level at the top half of SS-C BERs was significantly higher

than C-C BERs and control reactors in this experiment. The increment in DO was because of the O₂ gas produced at the stainless steel anode.

Prosnansky et al. (2005) recommended that extreme pH can be avoided by placing the anode upstream of a horizontal flow reactor while operating at current density below 12 A/m². With horizontal flow and upstream-anode design, the ORP and DO concerns also can be overcome by separating the anode and cathode zones with baffles. Larger reducing zone, or low ORP zone, can be created using cathode with larger surface area, and therefore plate-shaped instead of rod-shaped cathode is also recommended. The separation of anode and cathode zones using cation exchange membrane also would prevent the migration of NO₃⁻ ion to anode zone, thus allowing NO₃⁻ ion to remain in the cathode (reducing) zone for denitrification but still allowing H⁺ ions to enter reducing zone to neutralize OH⁻ ions (Park et al., 2005).

3.6 Supplementary Data

Methods for quantifying denitrifier - qPCR (Modified by Beth Douglass, NLAE)

Background: Our qPCR approach targets four denitrification genes; nirS, nirK (two different genes coding for the nitrite reductases: nirK, which codes for a Cu nitrite reductase and nirS, a cytochrome *cd1*-nitrite reductase; nosZI and nosZII (both genes coding for nitrous oxide reductase), the combination, however, covering a wider diversity in the bacterial communities of denitrifiers. For example, the primers we used initially for nosZI were described by Henry et al (2006) and have enjoyed widespread use. However, it has been known that these primers were not amplifying the entire bacterial community of denitrifiers, particularly the Bacteroidetes and the Firmicutes which have genera that are known to inhabit soil (Jones et al., 2013). Therefore we have provisionally adopted an approach that uses the primers described by Jones et al (2013) in addition to the nosZ1F and nosZ1R.

Equipment: MJ Research Opticon2 Thermal Cycler, Eppendorf Biophotometer

Primers:

Henry et al (2004) nirK with a 165 bp amplicon

nirK876 (F) – (5' ATY GGC GGV CAY GGC GA 3')

nirK1040 (R) – (5' GCC TCG ATC AGR TTR TGG TT 3')

Kandeler et al (2006) nirS with a 425 bp amplicon

nirSCd3aF – (5' AAC GYS AAG GAR ACS GG 3')

nirSR3cd – (5' GAS TTC GGR TGS GTC TTS AYG AA 3')

Henry et al (2006) amplify **Clade 1** denitrifiers with a 259 bp amplicon.

nosZ1F - (5' WCS YTG TTC MTC GAC AGC CAG 3')

nosZ1R - (5' ATG TCG ATC ARC TGV KCR TTY TC 3')

Jones et al. (2013) amplify **Clade 2** denitrifiers with a 620-720 bp amplicon.

nosZIIF (5' CTI GGI CCI YTK CAY AC 3')

nosZIIR (5' CGI GAR-CAR AAI TCB GTR C 3')

Fierer et al. (2005) amplify 16S-rRNA gene from *Bacteria* with a 200 bp amplicon

Eub 338 (5' ACT CCT ACG GGA GGC AGC AG 3')

Eub 518 (5' ATT ACC GCG GCT GCT GG 3')

Standards (nirK): We used *Rhizobium meliloti* (ATCC 9930) as the positive strain for standard DNA. A culture of *Rhizobium meliloti* was grown on YEM agar, colonies selected and grown in YEM broth and DNA was extracted (Qiagen's DNeasy Tissue KitTM (Qiagen, Valencia, CA, USA) as specified by the manufacturer). An environmental isolate, DN-3, from our collection was also used to generate DNA and used as template for the nirK gene; it was grown on nutrient agar and then nutrient broth culture prior to DNA extraction.

Standards (nirS): We used *Parococcus denitrificans* (ATCC 19367) and *Pseudomonas stutzeri* (ATCC 14405) as the positive strains for standard DNA. *P. nitrificans* was grown in nutrient broth grown in YEM broth and DNA was extracted (Qiagen's DNeasy Tissue KitTM (Qiagen, Valencia, CA, USA) as specified by the manufacturer).

nosZ I (Clade 1): We used *Pseudomonas stutzeri* (ATCC 14405) as the positive strain for standard DNA. A culture of *P. stutzeri* was grown overnight in marine broth and DNA was extracted (Qiagen's QIAamp DNA Mini Kit). Then qPCR** with nosZ1 primers was performed with and without SYBR-Green. The PCR products without SYBR-Green (used Qiagen HotStar Taq Plus* and increased the MgCl₂ concentration by 1.0 mM in the reaction) were cloned into pCR-4TOPO vector followed by transformation of One Shot TOP10 chemically competent *E.*

coli using the TOPO TA cloning kit (Invitrogen Cat No K4575-01). The resulting clones were tested by extracting plasmid DNA (5 PRIME FastPlasmid Mini-Prep Kit) and then performing qPCR** and gel electrophoresis to determine plasmid size.

nosZ II (Clade 2): A similar procedure was used to construct plasmids containing the PCR product amplified by nosZ-II primers. In this case, the nosZ DNA was amplified from *Geobacillus thermodenitrificans* (ATCC 29492). These plasmids containing their respective nosZ gene fragments were utilized as standards. By knowing the ratio of the size of the inserted gene fragment to the total size of the plasmid, DNA concentrations can be converted into gene copy numbers.

qPCR: Each qPCR run included positive standards (dilutions of plasmid DNA), and negative standards: water as template (no DNA) or E coli (ATCC 43651) genomic DNA. Each dilution of standard, and each negative control were prepared in triplicate wells of the 96 well PCR plate. Before dilution of the standards, the DNA concentration was determined using an Eppendorf Biophotometer.

Each reaction contained 12.5 μ L of 2X QuantiTect SYBR Green Master Mix (Qiagen), 5.0 μ L of 6.25 μ mol/L of each nosZ1 primer (or any combination of volume and concentration to result in 1.25 μ mol/L primer concentration in the well). The volume of standard or sample DNA was 2.5 μ L per well.

nosZ1 primers (Clade 1): Thermal cycling conditions included initial Taq polymerase activation at 95°C for 15 min and 40 cycles of 95°C for 15 s (denaturation), 53°C for 15 s (annealing), 72°C for 30s (extension), and 80°C for 15 s (data acquisition) followed by melting curve analysis from 50 to 90°C. We recommend that the annealing temperature be independently confirmed for each PCR machine because we have seen deviation from published values by as much as several degrees.

nosZII primers (Clade 2): Thermal cycling conditions included initial Taq polymerase activation at 95°C for 15 min and 40 cycles of 95°C for 30 s (denaturation), 47°C for 1 min (annealing), 72°C for 30 s (extension), followed by melting curve analysis from 50 to 98°C. Once again, we recommend that the annealing temperature be independently confirmed because of differences between thermocyclers.

nirK and nirS primers: Thermal cycling conditions included initial Taq polymerase activation at 95°C for 15 min followed by 5 cycles of touchdown sequence from 63°C to 59°C followed by 40 cycles with an annealing temp of 58 and melting curve analysis from 50 to 90°C as described by Henry, et al 2006.

References

- Fierer, N., JJ Jackson, R. Vilgalys & RB Jackson (2005) Assessment of soil microbial community structure by use of taxon-specific quantitative pcr assays. *Appl Environ Microbiol* 71: 4117-4120.
- Henry, S., D. Bru, B. Stres, S. Hallet & L. Philippot (2006) Quantitative detection of the nosZ gene, encoding nitrous oxide reductase, and comparison of the abundances of the 16S rRNA, narG, nirK and nosZ genes in soil. *Appl. Environ. Microbiol.* 72, 5181-5189.
- Henry, S., E. Baudoin, JC López-Gutiérrez, F. Martin-Laurent, A. Brauman & L. Philippot (2004) Quantification of denitrifying bacteria in soils by nirK gene targeted real-time PCR. *J Microbiol Meth* 59: 327-335.
- Jones CM, Graft DRH, Bru D, Philippot L and Hallin S (2013) The unaccounted yet abundant nitrous oxide-reducing microbial community: a potential nitrous oxide sink. *ISME J* 7: 417-426.
- Kandeler E, Deiglmayr K, Tschirko D, Bru D & Philippot L (2006) Abundance of narG, nirS, nirK, and nosZ Genes of Denitrifying Bacteria during Primary Successions of a Glacier Foreland. *Appl Environ Microbiol* 72: 5957–5962.

Table S1: Chemical constituents of synthetic nutrient solution

Chemical salt added	Chemical constituents	Conc. (mg/L)
CaCl ₂ *2H ₂ O	CaCl ₂	29.40
KH ₂ PO ₄	PO ₄ -P	0.50
H ₃ BO ₃	H ₃ BO ₃	1.55
MnSO ₄ *H ₂ O	MnSO ₄	0.34
ZnSO ₄ *7H ₂ O	ZnSO ₄	0.58
CuSO ₄	CuSO ₄	0.08
Na ₂ MoO ₄ *2H ₂ O	Na ₂ MoO ₄	0.12
Nitrates and Sulfates		
KNO ₃	NO ₃ -N	30.00
Sulfate from K₂SO₄ and MgSO₄		
MgSO ₄ *7H ₂ O	SO ₄ -S	5.00
K ₂ SO ₄	SO ₄ -S	5.00

Table S2: The mean \pm standard deviation of pH, ORP, and DO at each sampling location of each reactor.

Column	Sampling location	pH		ORP (mV)		DO (mg/L)		NO ₃ -N removal (%)	
		100 mA	500 mA	100 mA	500 mA	100 mA	500 mA	100 mA	500 mA
	Influent	5.1 \pm 0.1	5.3 \pm 0.5	447.8 \pm 38.9	359.5 \pm 79.6	7.9 \pm 0.2	7.9 \pm 0.3		
SS-C (1)	In-Col 1	6.9 \pm 3.1	9.4 \pm 1.7	294.4 \pm 210.4	27.6 \pm 146.0	1.7 \pm 0.2	1.8 \pm 0.4	16.7 \pm 4.8	25.8 \pm 13.0
	In-Col 2	5.4 \pm 3.8	6.4 \pm 1.6	369.9 \pm 236.5	131.2 \pm 113.2	2.4 \pm 0.1	2.3 \pm 1.6		
	In-Col 3	10.4 \pm 1	6.5 \pm 1.3	-57.8 \pm 156.8	79.1 \pm 78.7	2.4 \pm 1.4	2.7 \pm 1.3		
	Effluent	6.8 \pm 0.5	6.1 \pm 0.4	154.9 \pm 41.8	122.6 \pm 70.0	2.9 \pm 0.2	4.4 \pm 0.5		
SS-C (2)	In-Col 1	8.9 \pm 2.9	11.0 \pm 0.4	112.6 \pm 199.3	-28.4 \pm 233.3	1.5 \pm 0.1	2.2 \pm 0.6	16.5 \pm 5.4	20.7 \pm 10.8
	In-Col 2	5.6 \pm 2.2	10.5 \pm 1.1	304.4 \pm 198.3	-10.0 \pm 231.2	3.7 \pm 0.9	3.2 \pm 0.8		
	In-Col 3	10.0 \pm 1.1	5.0 \pm 1.8	115.6 \pm 82.1	30.3 \pm 127.6	2.3 \pm 0.7	3.7 \pm 0.8		
	Effluent	6.5 \pm 0.7	4.8 \pm 1.1	127.5 \pm 26.2	147.1 \pm 46.8	4.0 \pm 0.3	5.2 \pm 0.4		
C-C (1)	In-Col 1	9.0 \pm 3.0	9.9 \pm 1.7	46.9 \pm 312.0	-11.0 \pm 26.9	1.8 \pm 1.1	2.4 \pm 0.5	30.1 \pm 9.8	57.5 \pm 19.7
	In-Col 2	6.4 \pm 1.9	6.6 \pm 1.9	238.6 \pm 62.9	8.7 \pm 82.7	1.1 \pm 0.4	1.0 \pm 0.6		
	In-Col 3	6.1 \pm 0.7	5.3 \pm 1.0	258.3 \pm 35.0	181.9 \pm 100.6	1.3 \pm 0.1	1.3 \pm 0.2		
	Effluent	5.6 \pm 0.5	4.8 \pm 1.0	314.0 \pm 109.7	158.6 \pm 92.7	1.4 \pm 0.3	1.7 \pm 0.6		
C-C (2)	In-Col 1	7.3 \pm 2.8	5.7 \pm 2.6	304.4 \pm 95.7	306.2 \pm 96.0	1.7 \pm 0.5	1.2 \pm 0.2	10.6 \pm 7.0	25.7 \pm 8.9
	In-Col 2	5.6 \pm 1.4	4.5 \pm 2.9	347.4 \pm 53.1	332.4 \pm 105.0	1.5 \pm 0.4	1.0 \pm 0.3		
	In-Col 3	6.5 \pm 0.3	5.0 \pm 2.9	275.7 \pm 40.0	236.2 \pm 139.3	1.3 \pm 0.5	1.0 \pm 0.1		
	Effluent	5.5 \pm 0.4	5.4 \pm 0.7	297.7 \pm 14.0	120.1 \pm 88.4	1.5 \pm 0.2	1.6 \pm 0.4		
Control	In-Col 1	6.1 \pm 0.2	5.9 \pm 0.3	311.0 \pm 17.0	293.8 \pm 35.5	1.2 \pm 0.2	1.0 \pm 0.3	16.2 \pm 6.5	11.0 \pm 5.2
	In-Col 2	6.2 \pm 0.1	6.1 \pm 0.4	292.4 \pm 10.2	274.7 \pm 40.3	1.1 \pm 0.3	1.0 \pm 0.3		
	In-Col 3	6.3 \pm 0.1	6.1 \pm 0.4	264.9 \pm 42.4	261.8 \pm 58.7	1.2 \pm 0.2	1.0 \pm 0.3		
	Effluent	6.2 \pm 0.1	6.1 \pm 0.4	276.2 \pm 25.7	291.7 \pm 43.7	1.3 \pm 0.6	1.9 \pm 0.5		
Control	In-Col 1	6.1 \pm 0.1	5.9 \pm 0.4	333.7 \pm 60.2	325.1 \pm 46.5	1.0 \pm 0.3	1.4 \pm 0.3	20.7 \pm 7.2	12.0 \pm 5.0
	In-Col 2	6.2 \pm 0.1	6.1 \pm 0.4	342.7 \pm 76.9	313.8 \pm 40.4	1.0 \pm 0.1	1.0 \pm 0.4		
	In-Col 3	6.2 \pm 0.1	6.2 \pm 0.4	371.4 \pm 122.0	295.7 \pm 56.3	1.2 \pm 0.4	1.1 \pm 0.3		
	Effluent	6.3 \pm 0.1	6.1 \pm 0.3	304.5 \pm 10.1	278.3 \pm 49.7	0.9 \pm 0.1	1.2 \pm 0.5		

Table S3: Summary of *nosZ* and EUB gene abundance, and relative abundance of *nosZ* gene in BER and control reactors.

Column	Sample ID	Sampling location	EUB copies/gdw	<i>nosZ</i> copies/gdw	EUB log10/gdw	<i>nosZ</i> log10/gdw	<i>nosZ</i> rel abund
SS-C (1)	27	Inlet	1.27E+14	ND	14.10	ND	ND
	28	In-Col 1	9.84E+13	2.96E+12	13.99	12.47	3.0%
	26	In-Col 2	2.41E+13	ND	13.38	ND	ND
	30	In-Col 3	5.89E+13	2.48E+11	13.77	11.39	0.4%
	29	Outlet	1.01E+14	3.81E+11	14.00	11.58	0.4%
SS-C (2)	32	Inlet	1.27E+14	1.36E+12	14.10	12.13	1.1%
	33	In-Col 1	4.98E+13	2.03E+11	13.70	11.31	0.4%
	31	In-Col 2	1.70E+14	2.02E+11	14.23	11.31	0.1%
	35	In-Col 3	4.15E+12	ND	12.62	ND	ND
	34	Outlet	4.03E+13	5.06E+11	13.61	11.70	1.3%
C-C (1)	37	Inlet	3.10E+12	2.30E+10	12.49	10.36	0.7%
	38	In-Col 1	1.22E+13	6.33E+10	13.09	10.80	0.5%
	36	In-Col 2	8.12E+12	1.87E+10	12.91	10.27	0.2%
	40	In-Col 3	1.49E+13	3.15E+10	13.17	10.50	0.2%
	39	Outlet	1.11E+13	1.38E+10	13.05	10.14	0.1%
C-C (2)	42	Inlet	1.77E+13	7.12E+10	13.25	10.85	0.4%
	43	In-Col 1	2.24E+13	4.31E+10	13.35	10.63	0.2%
	41	In-Col 2	4.73E+12	2.69E+10	12.67	10.43	0.6%
	45	In-Col 3	4.06E+12	1.35E+10	12.61	10.13	0.3%
	44	Outlet	1.00E+13	1.56E+11	13.00	11.19	1.6%
Control (1)	47	Inlet	7.58E+13	1.62E+12	13.88	12.21	2.1%
	48	In-Col 1	1.52E+14	5.78E+11	14.18	11.76	0.4%
	46	In-Col 2	ND	1.31E+12	ND	12.12	ND
	50	In-Col 3	1.65E+14	3.02E+12	14.22	12.48	1.8%
	49	Outlet	1.36E+14	6.33E+11	14.13	11.80	0.5%
Control (2)	52	Inlet	1.33E+14	1.06E+12	14.12	12.03	0.8%
	53	In-Col 1	2.09E+14	1.42E+12	14.32	12.15	0.7%
	51	In-Col 2	9.27E+13	ND	13.97	ND	ND
	55	In-Col 3	1.32E+14	3.05E+11	14.12	11.48	0.2%
	54	Outlet	8.74E+13	3.11E+12	13.94	12.49	3.6%

Table S4: Sensitivity coefficient analysis of several key input costs. The values below showed the changes (%) in N removal cost by increasing 1% of respective costs.

Costs	Units	Base Case*	Scenario 1	Scenario 2	Scenario 3	Scenario 4
Capital cost						
Bioreactor (Excavation, structure, woodchips, etc.)	%	1.719	0.513	0.452	0.092	0.103
Cathodes (graphite)	%	0.000	0.232	0.204	0.041	0.047
Maintenance cost						
Anode (graphite/stainless)	%	0.000	0.224	0.316	0.175	0.072
Operating cost						
Electricity	%	0.000	0.246	0.216	0.730	0.821

APPENDIX A: PRELIMINARY EXPERIMENT

Overview

A preliminary experiment which introduced electrical stimulation into batch-scale woodchip bioreactors was conducted. Controlled conditions include temperature (room temperature), hydraulic retention time (HRT, 8 hours) and initial $\text{NO}_3\text{-N}$ concentration (30 mg/L). Alternatively, current intensity and electrode properties were manipulated to evaluate their effect on nitrate removal efficiency.

Materials and Methods

Electrode Properties and Anode-Cathode Combinations

The material of electrodes was chosen based on material nobility as shown in the galvanic corrosion chart (Zhang and Revie, 2011). Durability of electrode would directly affect the maintenance cost of the reactors, and therefore the materials that are more inert were chosen as electrodes. However, inert materials such as platinum, gold, and titanium were excluded in this experiment due to high capital cost. Consequently, graphite (C) and 316-stainless steel (SS) were chosen for testing. Meanwhile, aluminum (Al) which has high electrical conductivity was also tested for proof of concept of electrical stimulation despite of its low durability. The dimension of all electrodes was 2.6 inches (width) by 2.6 inches (height). The four pairs of electrodes (anode-cathode) that were tested include Al-Al, C-C, SS-SS and SS-C.

Experimental Set-up

300 g of air-dry woodchips were weighed (Denver Instrument TP-323) and placed into each 1000 mL beaker. Respective electrode pair were inserted into the beakers and connected to

power supply (ENDURO 300V). Distance between anode and cathode was kept relatively constant at approximately 2 inches. 600 mL of nutrient solution was then added into the beakers (will be referred as reactor). 100 mA current was supplied to the bio-electrochemical reactors to develop biofilm while allowing woodchips to be pre-saturated for 72 hours. A control reactor which did not receive electrical stimulation was also set up. Nutrient solution was replaced prior to batch testing. The effect of current intensity on nitrate removal was evaluated at 80 mA, 100 mA, 150 mA and 200 mA.

Sample Collection

50 mL water sample was collected from each reactor at the beginning of experiment. A subsample of 25 mL was used for $\text{NO}_3\text{-N}$ analysis, while the remaining 25 mL was used for pH analysis. After 8-hr HRT, 50 mL water sample was collected from the reactors. Similarly, 25 mL subsample was analyzed immediately for $\text{NO}_3\text{-N}$ concentration while the remaining sample was tested for pH.

Sample Analysis

For $\text{NO}_3\text{-N}$ analysis, both reaction zones of nitrate test strips (EMD Millipore) were immersed into 25 mL of sample for 1 second. The excess liquid from the strip was shaken off. After 1 minute, $\text{NO}_3\text{-N}$ concentration was determined by comparing the color of the top reaction zone with the provided color scale. However, if discoloration occurred at the bottom reaction zone (presence of nitrite ions), the sample was further treated. 5 drops of 10% aqueous amidosulfuric acid solution was added into 5 mL of sample and shook several times. Nitrate measurement was repeated after treatment. pH of the water sample was analyzed using portable meter (Orion 290A) probe.

Result and Discussion

Effect of Current Intensity on Nitrate Removal

All of the bio-electrochemical reactors (BER) followed a similar trend in nitrate removal efficiency when current intensity increased from 80 mA to 200 mA. The nitrate removal efficiency increased with increasing current intensity until the BERs achieved their respective peak current, then started to decline as the current intensity continued to increase. The Al-Al BER had the best nitrate removal (80%) at 80 mA and 100 mA. The best nitrate removal (50%) for C-C BER was found to be between 100 mA and 150 mA. Finally, the SS-SS (77%) and SS-C (40%) BERs had best nitrate removal efficiency at 150 mA and 100 mA, respectively. The control had the lowest nitrate removal efficiency at 17%. Few of the primary reasons that may contribute to the trend mentioned above were likely the oxygen and hydrogen gas production rate. In BER, oxygen gas was being produced at anode as a result from electrolysis of water. Although more electrons were provided to the denitrifier at higher current intensity, it is important to note that more oxygen gas was also produced, which could result in inhibition of denitrification. On the other hand, excessive production of hydrogen gas at cathode using high applied current was also known to cause inhibition effect on denitrification (Thrash and Coates, 2008).

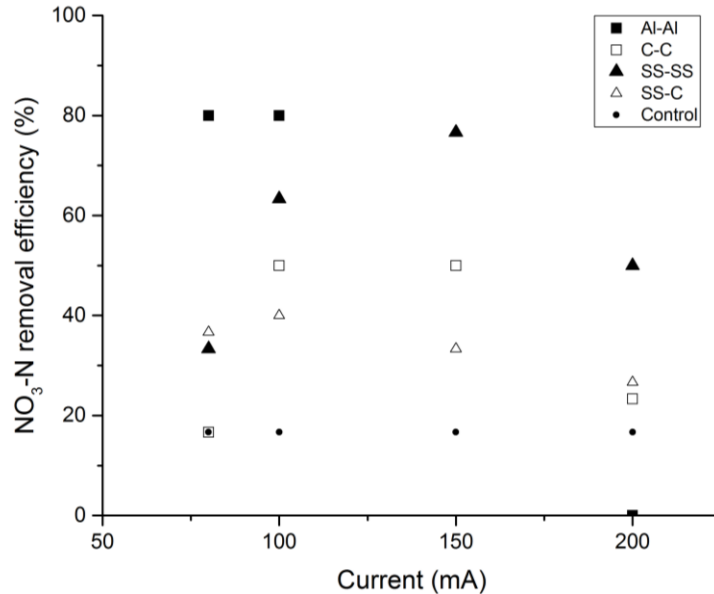


Figure A1: Nitrate removal of each electrode pair at 80, 100, 150 and 200 mA. Al = aluminum, C = graphite, SS = 316-stainless steel

Implication of Work

As shown in Figure A1, Al-Al BER demonstrated the highest nitrate removal efficiency at its peak current intensity. It was followed by SS-SS, C-C, and SS-C BERs at their respective peak current. Despite the exceptional nitrate removal efficiency in Al-Al BER, the degradation of Al anode was also the greatest due to its low corrosion resistant, which make this electrode pair impractical in long-term application. On the other hand, the SS-SS BER also demonstrated high nitrate removal efficiency, but the high cost of 316 stainless steel would likely cost-prohibitive in the full-scale reactors. Alternatively, the C-C and SS-C BERs, which had lower electrode costs, also exhibited higher nitrate removal efficiency than control woodchip reactors, and thus were chosen as the electrode pairs that will be tested in the column study.

APPENDIX B: RAW DATA

This table presents the NO₃-N concentrations in influent and effluents from Day 33 to Day 147 from the beginning (6/23/2016) of column experiment. Day 0-31 was flushing period; Day 32-70 experiment was tested using 100 mA current, 10°C and 5.9-hr HRT; Day 71-81 was transition period for temperature change from 10°C to 22.5°C. Day 82-128 experiment was tested using 500 mA current, 22.5°C and 8.2-hr HRT; Day 129-149 experiment was tested using 100 mA current, 22.5°C and 8.2-hr HRT. SS-C represents electrical treatment with stainless steel anode and carbon cathode; C-C represents electrical treatment with carbon anode and carbon cathode. Controls were simply woodchip bioreactors.

Date	Day from start-up	NO ₃ -N concentration (mg/L)						
		Influent	SS-C (1)	SS-C (2)	C-C (1)	C-C (2)	Control (1)	Control (2)
6/23/2016	0	ND	ND	ND	ND	ND	ND	ND
7/26/2016	33	29.19	26.52	28.35	25.76	24.87	27.74	29.22
7/27/2016	34	29.04	27.19	26.78	24.86	27.80	26.63	22.04
7/28/2016	35	22.06	28.32	25.49	29.06	26.75	28.86	32.86
7/29/2016	36	27.74	24.69	25.36	24.33	23.46	27.37	29.07
7/30/2016	37	19.59	30.34	28.58	30.02	28.52	33.49	36.60
8/4/2016	42	25.77	24.13	23.46	22.94	21.76	26.99	28.38
8/5/2016	43	28.50	26.38	26.85	25.32	25.78	26.98	28.87
8/6/2016	44	29.38	27.54	28.25	25.91	26.04	29.62	29.78
8/7/2016	45	ND	31.02	29.08	29.56	26.74	29.58	31.84
8/8/2016	46	20.29	ND	31.52	29.16	28.69	30.04	32.20
8/9/2016	47	24.41	ND	27.57	ND	22.99	27.10	26.87
8/10/2016	48	28.52	ND	26.57	26.33	24.03	26.10	27.11
8/11/2016	49	ND	ND	30.07	27.15	29.89	29.60	29.32
8/12/2016	50	30.32	ND	29.32	27.72	28.65	28.75	29.61
8/13/2016	51	27.75	ND	29.97	26.78	28.52	28.85	30.28
8/14/2016	52	20.98	ND	32.02	30.13	31.87	31.07	35.18
8/15/2016	53	28.24	ND	25.68	ND	24.19	26.89	27.20
8/17/2016	55	20.46	24.19	26.43	22.17	31.85	25.79	37.30
8/18/2016	56	26.73	27.22	26.28	27.38	25.97	26.26	29.45
8/19/2016	57	24.23	31.39	29.23	28.26	28.54	29.78	32.58
8/20/2016	58	29.67	27.27	29.45	25.97	24.38	29.36	27.43
8/21/2016	59	23.20	29.20	29.57	29.29	30.04	31.77	34.18
8/23/2016	61	26.04	27.61	26.64	26.05	26.00	29.27	28.84
8/24/2016	62	23.90	27.44	29.04	27.73	27.00	28.80	32.07
8/25/2016	63	23.43	28.05	27.72	27.73	27.94	30.40	33.24
8/26/2016	64	28.02	25.07	26.45	26.72	24.40	26.38	29.19
8/27/2016	65	25.57	32.28	33.61	29.74	28.56	31.10	31.21
8/29/2016	67	27.42	29.72	29.43	29.92	29.02	32.80	33.81

8/31/2016	69	28.98	28.17	27.56	27.54	25.74	28.46	28.89
9/1/2016	70	26.58	31.79	31.24	28.67	21.96	29.57	28.89
9/3/2016	72	28.90	27.17	27.45	23.46	15.29	24.43	27.43
9/5/2016	74	33.94	24.46	23.79	22.61	14.54	23.49	27.20
9/7/2016	76	30.00	19.43	23.07	ND	11.79	21.16	22.73
9/9/2016	78	30.17	21.81	22.82	20.18	13.17	20.98	24.49
9/11/2016	80	32.57	21.18	25.30	22.02	17.88	26.43	29.85
9/13/2016	82	29.42	19.86	18.98	12.58	19.02	24.62	25.83
9/17/2016	86	28.09	24.64	17.83	4.41	26.89	24.29	21.75
9/19/2016	88	29.30	25.74	21.28	20.91	22.12	25.89	26.72
9/21/2016	90	28.64	24.67	18.03	3.21	20.34	24.11	25.34
9/23/2016	92	29.96	24.20	20.55	2.76	19.67	25.59	25.47
9/26/2016	95	29.05	21.54	21.53	13.59	18.31	24.72	24.72
9/28/2016	97	28.71	16.91	24.99	18.40	19.14	22.68	25.11
9/30/2016	99	27.96	20.98	21.95	17.86	20.14	25.06	25.48
10/2/2016	101	ND	22.07	20.58	16.47	22.69	26.40	25.65
10/4/2016	103	29.04	16.49	25.34	14.56	21.12	26.58	25.40
10/6/2016	105	29.06	17.36	23.09	13.06	21.41	26.05	26.53
10/8/2016	107	28.71	16.66	23.32	13.58	21.49	25.50	25.33
10/10/2016	109	28.31	16.75	25.47	11.91	20.95	25.88	25.81
10/12/2016	111	23.54	20.21	25.48	13.33	26.69	27.25	25.69
10/14/2016	113	23.11	19.01	24.28	14.54	20.51	28.17	24.57
10/16/2016	115	26.73	18.63	21.68	11.40	21.71	25.83	24.25
10/20/2016	119	25.00	23.69	24.08	ND	22.78	26.84	26.39
10/22/2016	121	28.05	23.67	25.30	ND	19.64	25.27	23.55
10/24/2016	123	29.75	25.80	27.45	ND	22.86	27.77	24.33
10/26/2016	125	17.60	24.99	24.41	ND	29.90	29.30	25.09
10/28/2016	127	27.50	23.43	ND	22.22	20.88	25.77	23.94
10/30/2016	129	24.23	24.39	23.02	22.43	25.89	25.76	23.39
11/1/2016	131	14.32	24.58	17.75	21.62	30.42	28.79	26.25
11/3/2016	133	29.50	22.01	24.21	20.68	23.48	22.81	19.86
11/5/2016	135	26.41	22.86	24.90	21.65	26.48	25.40	24.16
11/7/2016	137	29.15	22.92	24.35	20.32	23.95	22.62	22.01
11/9/2016	139	28.76	23.80	23.55	20.90	25.38	23.37	21.55
11/11/2016	141	27.16	22.84	21.32	20.44	26.29	23.58	22.64
11/13/2016	143	28.02	23.75	21.54	20.49	25.42	22.24	21.55
11/15/2016	145	29.06	25.85	25.21	19.80	26.78	25.86	23.82
11/17/2016	147	29.05	25.00	24.48	13.97	24.83	24.11	24.00

Total Organic Carbon concentrations in influent and effluents. Samples from 7/2/2016 to 7/10/2016 were obtained during start-up period to determine the start-up TOC leaching. Samples from 8/26/2016 to 11/9/2016 were obtained to observe the TOC leaching in C-C treatment due to oxidation of carbon anode. SS-C represents electrical treatment with stainless steel anode and carbon cathode; C-C represents electrical treatment with carbon anode and carbon cathode. Controls were simply woodchip bioreactors.

Date	Total Organic Carbon concentration (ppm)						
	Influent	SS-C (1)	SS-C (2)	C-C (1)	C-C (2)	Control (1)	Control (2)
7/2/2016	ND	5.90	5.02	8.02	8.52	8.31	4.16
7/3/2016	ND	5.88	3.86	6.79	7.59	7.60	3.99
7/4/2016	ND	5.36	3.77	5.54	7.22	7.85	4.45
7/5/2016	ND	5.70	3.77	5.48	7.22	6.90	3.82
7/6/2016	ND	4.03	3.09	4.79	6.33	7.81	3.67
7/7/2016	ND	4.15	3.00	4.42	6.38	5.60	3.22
7/8/2016	ND	3.88	3.07	4.24	5.46	4.71	2.90
7/9/2016	ND	3.45	2.88	4.36	4.54	4.05	2.65
7/10/2016	ND	4.00	2.87	3.91	4.53	ND	2.46
8/26/2016	0.16	4.85	2.05	3.51	11.90	1.63	0.89
8/31/2016	0.10	3.18	1.87	3.49	10.41	1.03	0.77
9/21/2016	0.07	4.03	9.23	27.20	13.03	2.94	2.33
9/28/2016	0.21	6.92	7.77	15.43	8.02	2.50	2.05
10/20/2016	0.28	6.57	11.30	ND	7.05	2.01	2.30
11/2/2016	0.20	3.18	4.73	13.50	7.53	2.48	1.93
11/9/2016	0.27	2.44	3.37	7.87	4.01	2.37	2.06

pH, ORP, and DO data of influent nutrient solution.

Influent						
Date	Current (mA)	Temp (C)	HRT (hr)	pH	ORP	DO
28-Jul	100	10	8	5.63	453.6	9.38
31-Jul	100	10	8	5.74	429	9.87
4-Aug	100	10	8	5.6	517.2	10.03
19-Aug	100	10	8	5.33	477.4	8.47
24-Aug	100	10	8	5.15	454.1	10.43
15-Sep	500	22.5	12	5.16	290.7	7.84
30-Sep	500	22.5	12	4.74	435.7	8.19
6-Oct	500	22.5	12	5.58	310.1	7.46
13-Oct	500	22.5	12	5.87	335.6	8.33
27-Oct	500	22.5	12	5.25	354.1	7.44
5-Nov	100	22.5	12	5.18	496.9	7.88
10-Nov	100	22.5	12	5.13	417.4	7.81
17-Nov	100	22.5	12	5.04	495.9	7.88

pH, ORP, and DO data of SS-C (1). SS-C represents electrical treatment with stainless steel anode and carbon cathode.

SS-C (1)				In-Col 1			In-Col 2			In-Col 3			Effluent		
Date	Current (mA)	Temp (C)	HRT (hr)	pH	ORP	DO	pH	ORP	DO	pH	ORP	DO	pH	ORP	DO
28-Jul	100	10	8	9.87	-23.4	4.62	7.48	-170.7	3.01	9.13	-106.8	5.75	6.47	11.7	5.81
31-Jul	100	10	8	6.41	386.5	5.96	6.67	360.1	2.98	6.84	342.6	2.84	6	252.1	1.96
4-Aug	100	10	8	6.38	468.7	6.62	6.86	422.1	3.72	7	415.8	3.54	5.72	422	1.95
19-Aug	100	10	8	5.9	468.9	2.15	3.5	477.1	2.44	5.62	480.2	1.71	5.6	476.1	2.04
24-Aug	100	10	8	9.8	393.2	1.85	6.49	440.7	3.35	4.38	461.8	4.63	3.98	469.6	4.42
15-Sep	500	22.5	12	9.93	5.3	2.42	5.95	81.5	1.33	5.9	84.4	2.6	5.66	116.4	3.83
30-Sep	500	22.5	12	7.96	-66.8	1.71	4.86	116.7	5.07	5.38	138.8	4.72	6.18	237.1	4.3
6-Oct	500	22.5	12	10.92	-40.5	1.58	6.83	91.7	1.76	6.69	3.5	1.86	6.3	79.6	4.24
13-Oct	500	22.5	12	10.84	-44.7	1.42	9.03	38.8	1.5	8.73	-3.4	1.53	5.83	124.9	5.13
27-Oct	500	22.5	12	7.36	284.5	1.79	5.41	327.3	1.99	5.91	172	2.93	6.51	54.9	4.69
5-Nov	100	22.5	12	6.11	370	1.86	3.5	466	2.38	10.58	33.2	1.4	7.23	187.9	2.77
10-Nov	100	22.5	12	10.36	56.6	1.58	9.75	100.5	2.38	9.38	32.3	3.92	6.27	168.8	2.85
17-Nov	100	22.5	12	4.31	456.7	1.86	2.93	543.2	2.52	11.37	-238.8	1.79	6.79	107.9	3.13

pH, ORP, and DO data of SS-C (2). SS-C represents electrical treatment with stainless steel anode and carbon cathode.

SS-C (2)				In-Col 1			In-Col 2			In-Col 3			Effluent		
Date	Current (mA)	Temp (C)	HRT (hr)	pH	ORP	DO	pH	ORP	DO	pH	ORP	DO	pH	ORP	DO
26-Jul	100	10	8	10.04	ND	ND	5.749	ND	ND	5.568	ND	ND	6.32	ND	ND
30-Jul	100	10	8	10.37	-8.9	3.75	6.61	52.6	5.32	4.09	158.4	8.94	6.38	8.6	6.51
2-Aug	100	10	8	10.44	324	3.51	5.19	385.1	5.32	3.98	407.4	9.36	5.46	353.6	7.16
17-Aug	100	10	8	10.74	400.9	5.24	9.54	445.3	6.81	4.25	478.1	7.21	4.13	459	6.58
23-Aug	100	10	8	10.21	415.6	5.23	4.64	488.1	9.64	8.83	461	7.98	4.37	492.1	7.8
16-Sep	500	22.5	12	10.66	-200.5	1.78	8.76	-218.4	2.43	3.8	87.9	2.85	3.86	164.3	4.69
1-Oct	500	22.5	12	10.57	-191.9	2.35	10.14	-125.2	4.41	5.81	-181	2.8	4.23	200.9	5.42
6-Oct	500	22.5	12	11.52	-62.4	1.84	11.16	-55.4	3.01	7.63	18.8	4.03	6.17	102.6	5.07
14-Oct	500	22.5	12	11.38	-35.3	2.06	11.22	-34	2.77	4.59	153.9	4.74	5.72	93.6	5.68
28-Oct	500	22.5	12	11.05	348.3	3.15	11.03	383	3.28	3.18	71.9	3.82	4.03	174	5.11
6-Nov	100	22.5	12	10.52	50.7	1.46	6.83	216.2	4.35	8.83	24.7	2.77	6.22	155.9	3.86
11-Nov	100	22.5	12	5.56	335.5	1.63	3.1	531.5	2.61	10.93	138	1.46	7.25	122.3	3.73
17-Nov	100	22.5	12	10.67	-48.5	1.35	6.87	165.6	4.08	10.18	184.2	2.68	5.97	104.4	4.32

pH, ORP, and DO data of C-C (1). C-C represents electrical treatment with carbon anode and carbon cathode.

C-C (1)				In-Col 1			In-Col 2			In-Col 3			Effluent		
Date	Current (mA)	Temp (C)	HRT (hr)	pH	ORP	DO	pH	ORP	DO	pH	ORP	DO	pH	ORP	DO
28-Jul	100	10	8	9.44	224	5.35	5.54	314.7	3.38	5.96	255.3	2.59	6.18	-4.1	1.48
31-Jul	100	10	8	10.69	49.2	4.55	4.34	107.8	2.8	4.16	19.7	2.04	5.7	-32.1	1.73
4-Aug	100	10	8	10.32	311	4.74	4.88	351.1	2.93	4.15	364.2	1.82	5.61	356.1	1.98
19-Aug	100	10	8	9.01	428.4	4.66	3.74	453.3	2.21	3.48	440.2	2.03	5.59	450.1	2.84
24-Aug	100	10	8	8.78	398.5	5.45	5.6	424.6	2.91	3.04	432.7	2.39	4.82	427.6	2.49
15-Sep	500	22.5	12	10.19	-43.8	2.29	6.12	-108.9	0.7	4.68	17.5	1.21	4.65	38.1	1.83
30-Sep	500	22.5	12	9.83	-15.3	2.25	5.21	109.9	0.7	3.8	196.3	1.26	3.59	231.8	1.54
6-Oct	500	22.5	12	11.33	-7	2.84	6.98	55.1	0.83	5.83	170.7	1.09	5.49	104.1	1.08
13-Oct	500	22.5	12	11.12	30.3	2.89	9.56	12.1	0.83	6.38	271	1.31	6.08	265.9	1.42
27-Oct	500	22.5	12	7.12	-19.2	1.67	4.99	-24.7	2.04	5.67	254	1.53	3.94	153	2.68
5-Nov	100	22.5	12	10.02	146.6	2.98	8.48	201.9	1.59	6.68	298.7	1.28	6.08	204.3	1.14
10-Nov	100	22.5	12	5.58	296.8	0.77	4.76	311.3	0.78	6.2	238.9	1.17	5.08	423.6	1.65
17-Nov	100	22.5	12	11.24	-302.8	1.57	6.08	202.7	1.04	5.4	237.3	1.42	5.5	314	1.395

pH, ORP, and DO data of C-C (2). C-C represents electrical treatment with carbon anode and carbon cathode.

C-C (2)				In-Col 1			In-Col 2			In-Col 3			Effluent		
Date	Current (mA)	Temp (C)	HRT (hr)	pH	ORP	DO	pH	ORP	DO	pH	ORP	DO	pH	ORP	DO
26-Jul	100	10	8	7.30	ND	ND	5.561	ND	ND	3.85	ND	ND	5.37	ND	ND
30-Jul	100	10	8	6.65	18.8	2.84	5.8	-135	1.53	3.34	19.7	1.32	5.94	-74.7	1.54
2-Aug	100	10	8	6.6	357	2.82	6.58	338	1.54	3.59	373.8	1.49	4.84	362.1	1.31
17-Aug	100	10	8	4.69	430	3.83	6.78	420.8	2.08	4.01	427.1	1.87	5.3	422.3	2.08
23-Aug	100	10	8	9.89	387.9	3.32	6.62	414.4	1.52	5.71	418.4	1.4	5.04	424.8	1.73
16-Sep	500	22.5	12	9.77	182.6	1.02	9.28	182.2	0.92	9.89	47.8	0.94	4.37	-23.6	1.93
1-Oct	500	22.5	12	5.06	302.9	1.52	2.69	389.9	0.95	2.85	228.3	1.02	5.1	97.8	1
6-Oct	500	22.5	12	6.26	249.7	1.09	4.81	265.2	0.68	5.55	167.7	0.97	5.54	186.8	2.02
14-Oct	500	22.5	12	3.87	369.9	1.02	2.89	390.7	1.09	3.52	334.9	1.19	6.08	150.7	1.54
28-Oct	500	22.5	12	3.27	425.8	1.35	2.63	433.9	1.37	3.13	402.4	1.1	5.86	188.8	1.28
6-Nov	100	22.5	12	5.53	308.2	1.2	4.14	344.5	1.08	6.67	230.3	1.07	5.17	295.2	1.26
11-Nov	100	22.5	12	10.49	208.3	2.14	6.9	295.9	1.92	6.59	306	1.86	6	312.7	1.51
17-Nov	100	22.5	12	5.84	399.7	1.6	5.66	401.9	1.55	6.12	290.7	0.95	5.46	285.1	1.58

pH, ORP, and DO data of Control (1). Control was woodchip bioreactor.

Control (1)				In-Col 1			In-Col 2			In-Col 3			Effluent		
Date	Current (mA)	Temp (C)	HRT (hr)	pH	ORP	DO	pH	ORP	DO	pH	ORP	DO	pH	ORP	DO
28-Jul	100	10	8	6.06	387.7	2.04	6.33	348.1	1.07	6.29	340.4	0.8	6.25	326.2	1.62
31-Jul	100	10	8	6.02	423.1	1.99	6.22	377.7	1.43	6.29	372.7	1.48	6.34	322.3	1.65
4-Aug	100	10	8	5.86	427.1	2.57	6.09	421.8	1.34	6.14	401.1	1.12	6.13	392.5	1.04
19-Aug	100	10	8	5.68	437.6	1.31	5.9	431.9	0.98	5.93	436.7	1.06	5.87	438	1.14
24-Aug	100	10	8	5.51	421.1	1.47	5.86	422	1.57	5.84	424.3	1.52	5.81	428.7	2.69
15-Sep	500	22.5	12	5.68	328.6	0.83	5.86	287.5	0.94	5.83	282.8	0.8	5.89	291.3	2.76
30-Sep	500	22.5	12	5.4	269.1	0.97	5.63	249	0.66	5.6	217.3	1.15	5.58	313.7	1.91
6-Oct	500	22.5	12	6.17	261.8	0.88	6.44	230.9	1.25	6.45	194.3	1.42	6.26	240.7	1.46
13-Oct	500	22.5	12	6.12	273.7	0.72	6.39	270.3	0.8	6.35	270.9	0.88	6.69	261	1.56
27-Oct	500	22.5	12	6.04	336	1.37	6.28	335.7	1.39	6.21	343.9	0.84	6.11	351.8	1.91
5-Nov	100	22.5	12	6.17	325.4	1.16	6.26	303.7	0.76	6.22	298.6	0.89	6.27	298.4	1.2
10-Nov	100	22.5	12	6.23	292.2	0.97	6.29	289.6	1.08	6.35	278.7	1.28	6.27	248.1	0.7
17-Nov	100	22.5	12	5.93	315.3	1.42	6.17	283.9	1.38	6.18	217.3	1.32	6.18	282	1.85

pH, ORP, and DO data of Control (2). Control was woodchip bioreactor.

Control (2)				In-Col 1			In-Col 2			In-Col 3			Effluent		
Date	Current (mA)	Temp (C)	HRT (hr)	pH	ORP	DO	pH	ORP	DO	pH	ORP	DO	pH	ORP	DO
26-Jul	100	10	8	5.55	ND	2.27	5.755	ND	1.11	5.78	ND	1.09	5.86	ND	1.35
30-Jul	100	10	8	6.17	389.9	2.39	6.27	325.1	0.98	6.26	317.3	1.84	6.22	198.4	1.58
2-Aug	100	10	8	5.79	384.3	2.24	6.32	352.2	1.88	6.12	400.5	1.25	6.14	393.6	0.86
17-Aug	100	10	8	5.66	401.5	1.76	5.68	392.8	2.15	5.93	396.6	1.78	5.88	424.1	1.54
23-Aug	100	10	8	5.49	426.4	1.87	5.85	421.4	1.24	5.86	427.7	1.22	5.83	432	1.92
16-Sep	500	22.5	12	5.54	308.4	1.05	5.73	305.9	0.9	5.81	255.2	0.74	5.78	289	2.02
1-Oct	500	22.5	12	5.33	355.1	1.22	5.54	343.6	1.58	5.65	301.5	0.71	5.68	284.7	1.19
6-Oct	500	22.5	12	6.09	277.5	1.53	6.39	270.3	0.81	6.48	245.2	1.14	6.42	211.1	0.76
14-Oct	500	22.5	12	6.26	294.3	1.76	6.39	283.1	1.2	6.44	289.1	1.35	6.34	258.7	0.81
28-Oct	500	22.5	12	6.02	390.2	1.34	6.28	366.2	0.69	6.37	387.3	1.46	6.29	347.8	1.24
6-Nov	100	22.5	12	6.07	291.8	0.72	6.3	289.3	0.98	6.35	291	1.04	6.32	292.9	0.91
11-Nov	100	22.5	12	6.15	306.6	1.24	6.23	308.1	1.12	6.22	311.3	0.95	6.16	310.1	0.77
17-Nov	100	22.5	12	5.98	402.6	1.04	6.15	430.8	0.95	6.1	511.8	1.62	6.27	310.6	0.91

Denitrifier gene (*NosZ*) abundances in each treatment and control. SS-C represents electrical treatment with stainless steel anode and carbon cathode; C-C represents electrical treatment with carbon anode and carbon cathode. Controls were simply woodchip bioreactors.

Column	Sample ID	Sampling location	EUB	<i>NosZ</i>	EUB	<i>NosZ</i>	<i>NosZ</i>
			copies/gdw	copies/gdw	log10/gdw	log10/gdw	rel abund
SS-C (1)	27	Inlet	1.27E+14	ND	14.10	ND	ND
	28	In-Col 1	9.84E+13	2.96E+12	13.99	12.47	3.0%
	26	In-Col 2	2.41E+13	ND	13.38	ND	ND
	30	In-Col 3	5.89E+13	2.48E+11	13.77	11.39	0.4%
	29	Outlet	1.01E+14	3.81E+11	14.00	11.58	0.4%
SS-C (2)	32	Inlet	1.27E+14	1.36E+12	14.10	12.13	1.1%
	33	In-Col 1	4.98E+13	2.03E+11	13.70	11.31	0.4%
	31	In-Col 2	1.70E+14	2.02E+11	14.23	11.31	0.1%
	35	In-Col 3	4.15E+12	ND	12.62	ND	ND
	34	Outlet	4.03E+13	5.06E+11	13.61	11.70	1.3%
C-C (1)	37	Inlet	3.10E+12	2.30E+10	12.49	10.36	0.7%
	38	In-Col 1	1.22E+13	6.33E+10	13.09	10.80	0.5%
	36	In-Col 2	8.12E+12	1.87E+10	12.91	10.27	0.2%
	40	In-Col 3	1.49E+13	3.15E+10	13.17	10.50	0.2%
	39	Outlet	1.11E+13	1.38E+10	13.05	10.14	0.1%
C-C (2)	42	Inlet	1.77E+13	7.12E+10	13.25	10.85	0.4%
	43	In-Col 1	2.24E+13	4.31E+10	13.35	10.63	0.2%
	41	In-Col 2	4.73E+12	2.69E+10	12.67	10.43	0.6%
	45	In-Col 3	4.06E+12	1.35E+10	12.61	10.13	0.3%
	44	Outlet	1.00E+13	1.56E+11	13.00	11.19	1.6%
Control (1)	47	Inlet	7.58E+13	1.62E+12	13.88	12.21	2.1%
	48	In-Col 1	1.52E+14	5.78E+11	14.18	11.76	0.4%
	46	In-Col 2	ND	1.31E+12	ND	12.12	ND
	50	In-Col 3	1.65E+14	3.02E+12	14.22	12.48	1.8%
	49	Outlet	1.36E+14	6.33E+11	14.13	11.80	0.5%
Control (2)	52	Inlet	1.33E+14	1.06E+12	14.12	12.03	0.8%
	53	In-Col 1	2.09E+14	1.42E+12	14.32	12.15	0.7%
	51	In-Col 2	9.27E+13	ND	13.97	ND	ND
	55	In-Col 3	1.32E+14	3.05E+11	14.12	11.48	0.2%
	54	Outlet	8.74E+13	3.11E+12	13.94	12.49	3.6%

References

- Bard, A. J., and L. R. Faulkner (2001). *Electrochemical methods : fundamentals and applications*. 2nd ed. John Wiley & Sons, Inc. Hoboken, New Jersey. pg. 833.
- Beaudet, N., A. Otter, C. Karr, A. Perkins, and S. Sathyanarayana. (2014). Nitrates, Blue Baby Syndrome, and Drinking Water: A Factsheet for Families.
- Bell, N., and R. Cooke (2015). Characterizing the Performance of Denitrifying Bioreactors during Simulated Subsurface Drainage Events. *Journal of Environmental Quality* **44** (2015): pg.1647-1656. doi:10.2134/jeq2014.04.0162
- Carlson, B., J. Vetsch, and G. Randall. (2013). Nitrates in Drainage Water in Minnesota.
- Casella, S., and W. Payne (1996). Potential of denitrifiers for soil environment protection
- Cast, K., and J. Flora (1998). An evaluation of two cathode materials and the impact of copper on bioelectrochemical denitrification. *Water Research* **32** (1): pg.63-70.
- Christianson, L., A. Bhandari, M. Helmers, K. Kult, T. Sutphin, and R. Wolf (2012). Performance Evaluation of Four Field-Scale Agricultural Drainage Denitrification Bioreactors in Iowa. *Transactions of the Asabe* **55** (6): pg.2163-2174.
- Christianson, L., and M. Helmers. (2011). Woodchip Bioreactors for Nitrate in Agricultural Drainage.
- Christianson, L., J. Tyndall, and M. Helmers (2013). Financial comparison of seven nitrate reduction strategies for Midwestern agricultural drainage. *Water Resources and Economic* **2-3** (2013): pg.30-56. doi:<http://dx.doi.org/10.1016/j.wre.2013.09.001>
- Des Moines Water Works (2014). High Nitrate Levels in Des Moines and Raccoon Rivers Force Des Moines Water Works to Start the Nitrate Removal Facility. Available at: <http://www.dmww.com/about-us/announcements/high-nitrate-levels-in-des-moines-and-raccoon-rivers-force-des-moines-water-works-to-start-the-nitra.aspx>. Accessed 6/16/2017
- Diaz, R., and R. Rosenberg (2008). Spreading dead zones and consequences for marine ecosystems. *Science* **321** (5891): pg.926-929. doi:10.1126/science.1156401
- Diaz, R., and A. Solow (1999). *Ecological and Economic Consequences of Hypoxia*. National Oceanic and Atmospheric Administration.
- Dinnes, D., D. Karlen, D. Jaynes, T. Kaspar, J. Hatfield, T. Colvin, and C. Cambardella (2002). Nitrogen Management Strategies to Reduce Nitrate Leaching in Tile-Drained Midwestern Soils. *Agronomy Journal* **94** pg.153-171.
- EPA (2015). Northern Gulf of Mexico Hypoxic Zone. Available at: <https://www.epa.gov/ms-htf/northern-gulf-mexico-hypoxic-zone>. Accessed July 12th, 2017
- ESA. E. S. o. America. (2012). Hypoxia.
- Feleke, Z., K. Araki, Y. Sakakibara, T. Watanabe, and M. Kuroda (1998). Selective reduction of nitrate to nitrogen gas in a Biofilm electrode reactor. *Water Research* **32** (9): pg.2728-2734.
- Feyereisen, G., T. Moorman, L. Christianson, R. Venterea, J. Coulter, and U. Tschirner (2016). Performance of Agricultural Residue Media in Laboratory Denitrifying Bioreactors at Low Temperatures. *Journal of Environmental Quality* **45** (2016): pg.779-787. doi:10.2134/jeq2015.07.0407
- Flora, J. R., M. T. Suidan, S. Islam, P. Biswas, and Y. Sakakibara (1994). Numerical Modeling of a Biofilm-electrode Reactor Used for Enhanced Denitrification. *Water Science & Technology* **29** (10-11): pg.517-524.
- Follett, R. (1995). Fort Collins, Colorado: USDA Agricultural Research Service.

- Ghane, E., N. Fausey, and L. Brown (2014). Modeling nitrate removal in a denitrification bed. *Water Research* **71** (2015): pg.294-305.
doi:<http://dx.doi.org/10.1016/j.watres.2014.10.039>
- Gibert, O., S. Pomierny, I. Rowe, and R. Kalin (2008). Selection of organic substrates as potential reactive materials for use in a denitrification permeable reactive barrier (PRB). *Bioresource Technology* **99** (2008): pg.7587-7596. doi:10.1016/j.biortech.2008.02.012
- Gomez, M. A., E. Hontoria, and J. Gonzalez-Lopez (2001). Effect of dissolved oxygen concentration on nitrate removal from groundwater using denitrifying submerged filter. *Journal of Hazardous Materials* **B90** (2002): pg.267-278.
- Greenan, C., T. Moorman, T. Kaspar, T. Parkin, and D. Jaynes (2006). Comparing Carbon Substrates for Denitrification of Subsurface Drainage Water. *Journal of Environmental Quality* **35** pg.824-829. doi:10.2134/jeq2005.0247
- Greenan, C., T. Moorman, T. Parkin, T. Kaspar, and D. Jaynes (2009). Denitrification in Wood Chip Bioreactors at Different Water Flows. *Journal of Environmental Quality* **38** pg.1664-1671. doi:10.2134/jeq2008.0413
- Gregory, K., D. Bond, and D. Lovley (2004). Graphite electrodes as electron donors for anaerobic respiration. *Environmental Microbiology* **6** (6): pg.596-604.
doi:10.1111/j.1462-2920.2004.00593.x
- Hao, R. X., S. M. Li, J. B. Li, and C. C. Meng (2013). Denitrification of simulated municipal wastewater treatment plant effluent using a three-dimensional biofilm-electrode reactor: Operating performance and bacterial community. *Bioresource Technology* **143** pg.178-186. doi:10.1016/j.biortech.2013.06.001
- Hofmann, B., S. Brouder, and R. Turco (2004). Tile spacing impacts on Zea mays L. yield and drainage water nitrate load. *Ecological Engineering* **23** (2004): pg.251-267.
doi:10.1016/j.ecoleng.2004.09.008
- Hoover, N. (2012). Denitrification woodchip bioreactor two-phase column study: evaluation of nitrate removal at various hydraulic retention times and effect of temperature on denitrification rates. MS thesis. Ames, Iowa. Iowa State University, Environmental Science, Sustainable Agriculture
- Hoover, N., A. Bhandari, M. Soupir, and T. Moorman (2015). Woodchip Denitrification Bioreactors: Impact of Temperature and Hydraulic Retention Time on Nitrate Removal. *Journal of Environmental Quality* (Special section). doi:10.2134/jeq2015.03.0161
- Howarth, R., and R. Marino (2006). Nitrogen as the limiting nutrient for eutrophication in coastal marine ecosystems: Evolving views over three decades. *Limnology and Oceanography* **51** (1, part 2): pg.364-376.
- Hypoxia Task Force (2013). *Reassessment 2013 Assessing Progress Made Since 2008*. U.S. Environmental Protection Agency.
- IDALS Iowa (Department of Agriculture and Land Stewardship), Iowa Department of Natural Resources, Iowa State University College of Agriculture and Life Sciences (2013). Iowa Nutrient Reduction Strategy.
- Ikenberry, C., M. Soupir, K. Schilling, C. Jones, and A. Seeman (2014). Nitrate-Nitrogen Export: Magnitude and Patterns from Drainage Districts to Downstream River Basins. *Journal of Environmental Quality* **43** pg.2024-2033. doi:10.2134/jeq2014.05.0242
- Ilhan, E., S. K. Ong, and T. Moorman (2012). Herbicide and Antibiotic Removal by Woodchip Denitrification Filters: Sorption Processes. *Water Air and Soil Pollution* **223** pg.2651-2662. doi:10.1007/s11270-011-1057-5

- Ilhan, Z. E., S. K. Ong, and T. B. Moorman (2011). Dissipation of Atrazine, Enrofloxacin, and Sulfamethazine in Wood Chip Bioreactors and Impact on Denitrification. *Journal of Environmental Quality* **40** (2011): pg.1816-1823.
- IPNI. International Plant Nutrition Institute. (2016). Nitrogen Notes (Number 5).
- Jing, D., W. Li, Q.-L. Zhao, K. Wang, Z. Zheng, and Y.-Z. Gao (2015). Electroreduction of nitrate in water: Role of cathode and cell configuration. *Chemical Engineering Journal* **271** (2015): pg.252-259. doi:<http://dx.doi.org/10.1016/j.cej.2015.03.001>
- Kalita, P., R. Cooke, S. Anderson, and J. Mitchell (2007). Subsurface Drainage and Water Quality: The Illinois Experience. *Transactions of the Asabe* **50** (5): pg.1651-1556.
- Kandeler, E., K. Deiglmayr, D. Tschirko, D. Bru, and L. Philippot (2006). Abundance of narG, nirS, nirK, and nosZ Genes of Denitrifying Bacteria during Primary Successions of a Glacier Foreland. *Applied and Environmental Microbiology* **72** (9): pg.5957-5962.
- Karnauskas, M., M. Schirripa, C. Kelble, G. Cook, and K. Craig (2013). *Ecosystem Status Report for The Gulf of Mexico*. U.S. Department of Commerce.
- Lawlor, P., M. Helmers, J. Baker, S. Melvin, and D. Lemke (2008). Nitrogen Application Rate Effect on Nitrate-Nitrogen Concentration and Loss in Subsurface Drainage for an Corn-Soybean Rotation. *Transactions of the Asabe* **51** (1): pg.83-94.
- Li, M., C. Feng, Z. Zhang, and N. Suguira (2009). Efficient electrochemical reduction of nitrate to nitrogen using Ti/IrO₂-Pt anode and different cathodes. *Electrochimica Acta* **54** pg.4600-4606. doi:10.1016/j.electacta.2009.03.064
- Long, L., L. Schipper, and D. Bruesewitz (2011). Long-term nitrate removal in a denitrification wall. *Agriculture, Ecosystems and Environment* **140** (2011): pg.514-520. doi:10.1016/j.agee.2011.02.005
- Lovley, D., J. D. Coates, E. Blunt-Harris, E. Phillips, and J. Woodward (1996). Humic substances as electron acceptors for microbial respiration. *Nature* **382** pg.445-448.
- Lovley, D., J. Fraga, J. D. Coates, and E. Blunt-Harris (1999). Humics as an electron donor for anaerobic respiration. *Environmental Microbiology* **1** (1): pg.89-98.
- Manassaram, D., L. Backer, and D. Moll (2005). A Review of Nitrates in Drinking Water: Maternal Exposure and Adverse Reproductive and Developmental Outcomes. *Environmental Health Perspectives* **114** (3): pg.320-327. doi:10.1289/ehp.8407
- Mania, D., K. Heylen, R. Spanning, and A. Frostegard (2016). Regulation of nitrogen metabolism in the nitrateammonifying soil bacterium *Bacillus vireti* and evidence for its ability to grow using N₂O as electron acceptor. *Environmental Microbiology* **18** (9): pg.2937-2950. doi:10.1111/1462-2920.13124
- Mateju, V. C., Simona, Krejci, Jakub; Janoch, Tomas; (1992). Biological water denitrification - A review. *Enzyme and Microbial Technology* **14** pg.170-183.
- McCorvie, M., and C. Lant (1993). Drainage District Formation and the Loss of Midwestern Wetlands, 1850-1930. *Agricultural History* **67** (4): pg.13-39.
- Melodi, S., and H. Jason (2014, 5 August) "Gulf of Mexico 'dead zone' is the size of Connecticut". *Cable News Network*, Retrieved from <http://www.cnn.com/2014/08/05/tech/gulf-of-mexico-dead-zone/>.
- Mississippi River/Gulf of Mexico Hypoxia Task Force (2012). Hypoxia 101. Available at: <https://www.epa.gov/ms-htf/hypoxia-101>. Accessed 15 April, 2016
- Moorman, T., T. Parkin, T. Kaspar, and D. Jaynes (2010). Denitrification activity, wood loss, and N₂O emissions over 9 years from a woodchip bioreactor. *Ecological Engineering* **36** (2010): pg.1567-1574. doi:10.1016/j.ecoleng.2010.03.012

- Nadelhoffer, K. J. (1990). Microlysimeter for Measuring Nitrogen Mineralization and Microbial Respiration in Aerobic Soil Incubations. *Soil Science Society of American Journal* **54** pg.411-415.
- NHDES. New Hampshire Department of Environmental Services. (2006). Environmental Fact Sheet. *ARD-EHP-16*
- Painter, H. A. (1970). A review of literature on inorganic nitrogen metabolism in microorganisms. *Water Research Pergamon Press* **2** pg.415-425.
- Park, H. I., D. k. Kim, Y.-J. Choi, and D. Pak (2005). Nitrate reduction using an electrode as direct electron donor in a biofilm-electrode reactor. *Process Biochemistry* **40** (10): pg.3383-3388. doi:<http://dx.doi.org/10.1016/j.procbio.2005.03.017>
- Parkin, T., A. Sexstone, and J. Tiedje (1985). Adaptation of Denitrifying Populations to Low Soil pH. *Applied and Environmental Microbiology* **49** (5): pg.1053-1056.
- Prosnansky, M., Y. Sakakibara, and M. Kuroda (2002). High-rate denitrification and SS rejection by biofilm-electrode reactor (BER) combined with microfiltration. *Water Research* **36** (2002): pg.4801-4810. doi:S0043-1354(02)00206-3
- Prosnansky, M., Y. Watanabe, and M. Kuroda (2005). Comparative study on the bio-electrochemical denitrification equipped with a multi-electrode system. *Water Science & Technology* **52** (10-11): pg.479-485.
- Ranaivoson, A., J. Moncrief, R. Venterea, P. Rice, and M. Dittrich (2012). *Anaerobic Woodchip Bioreactor for Denitrification, Herbicide Dissipation and Greenhouse Gas Mitigation*. University of Minnesota, Minnesota Department of Agriculture.
- Randall, G., D. Huggins, M. Russelle, D. Fuchs, W. Nelson, and J. Anderson (1997). Nitrate Losses through Subsurface Tile Drainage in Conservation Reserve Program, Alfalfa, and Row Crop Systems. *Journal of Environmental Quality* **26** pg.1240-1247.
- Robertson, W., J. Vogan, and P. Lombardo (2008). Nitrate Removal Rates in a 15-Year-Old Permeable Reactive Barrier Treating Septic System Nitrate. *Ground Water Monitoring & Remediation* **28** (3): pg.65-72.
- Robertson, W. D. (2010). Nitrate removal rates in woodchip media of varying age. *Ecological Engineering* **36** (2010): pg.1581-1587. doi:10.1016/j.ecoleng.2010.01.008
- Ruark, M., S. Brouder, and R. Turco (2009). Dissolved Organic Carbon Losses from Tile Drained Agroecosystems. *Journal of Environmental Quality* **38** pg.1205-1215. doi:10.2134/jeq2008.0121
- Sakakibara, Y., and M. Kuroda (1993). Electric Prompting and Control of Denitrification. *Biotechnology and Bioengineering* **42** pg.535-537.
- Sakakibara, Y., and T. Nakayama (2001). A Novel Multi-Electrode System for Electrolytic and Biological Water Treatments: Electric Charge Transfer and Application to Denitrification. *Water Research* **35** (3): pg.768-778. doi:S0043-1354(00)00327-4
- Saleh-Lakha, S., K. Shannon, S. Henderson, C. Goyer, J. Trevors, B. Zebarth, and D. Burton (2009). Effect of pH and Temperature on Denitrification Gene Expression and Activity in *Pseudomonas mandelii*. *American Society for Microbiology* **75** (12): pg.3903-3911. doi:10.1128/AEM.00080-09
- Schipper, L., W. Robertson, A. Gold, D. Jaynes, and S. Cameron (2010). Denitrifying bioreactors - An approach for reducing nitrate loads to receiving waters. *Ecological Engineering* **36** (2010): pg.1532-1543. doi:10.1016/j.ecoleng.2010.04.008

- Schipper, L., and M. Vojvodic-Vukovic (2001). Five Years of Nitrate Removal, Denitrification and Carbon Dynamics in a Denitrification Wall. *Water Research* **35** (14): pg.3473-3477. doi:S0043-1354(01)00052-5
- Simek, M., and J. E. Cooper (2002). The influence of soil pH on denitrification: progress towards the understanding of this interaction over the last 50 years. *European Journal of Soil Science* **53** pg.345-354.
- Snoeyink, V. J., David (1980). *Water Chemistry*. John Wiley & Sons. New York. pg. 407-409.
- Tan, C., F. Ma, and S. Qiu (2013). Impact of carbon to nitrogen ratio on nitrogen removal at a low oxygen concentration in a sequencing batch biofilm reactor. *Water Science and Technology* **67** (3): pg.612-618. doi:10.2166/wst.2012.554
- The Nature Conservancy (2011). The Floods' Lingering Effects: New Study Shows Gulf "Dead Zone" One of the Largest on Record. Available at: <https://www.nature.org/ourinitiatives/regions/northamerica/areas/gulfofmexico/explore/gulf-of-mexico-dead-zone.xml>. Accessed 23 September, 2016
- Thrash, J. C., and J. D. Coates (2008). Review: Direct and indirect electrical stimulation of microbial metabolism. *Environmental Science & Technology* **42** (11): pg.3921-3931. doi:10.1021/es702668w
- Thrash, J. C., I. V. J. Trump, K. Weber, Miller, Elisabeth, L. Achenbach, and J. D. Coates (2007). Electrochemical Stimulation of Microbial Perchlorate Reduction. *Environmental Science & Technology* **41** pg.1740-1746. doi:10.1021/es062772m
- Tiedje, J. (1994). *Methods of Soil Analysis. Part 2, Microbiological and biochemical properties* Soil Science Society of America book series no. 5. Soil Science Society of America Madison, WI. pg. 245-267.
- USEPA US Environmental Protection Agency, (2012). *Water: Monitoring & Assessment - Nitrates*. Available at: <https://archive.epa.gov/water/archive/web/html/vms57.html>. Accessed 18 Oct 2015
- USEPA (2014). *Basic Information about Nitrate in Drinking Water*. Available at: <http://water.epa.gov/drink/contaminants/basicinformation/nitrate.cfm>. Accessed 13 October 2015
- USGS (2014). *Nitrate in the Mississippi River and its tributaries, 1980 to 2010: Are we making progress?* United States Geological Survey.
- Wang, J. H., B. C. Baltzis, and G. A. Lewandowski (1995). Fundamental Denitrification Kinetic Studies with *Pseudomonas denitrificans*. *Biotechnology and Bioengineering* **47** pg.26-41.
- Warneke, S., L. Schipper, M. Matiasek, K. Scow, S. Cameron, D. Bruesewitz, and I. McDonald (2011a). Nitrate removal, communities of denitrifiers and adverse effects in different carbon substrates for use in denitrification beds. *Water Research* **45** pg.5463-5475. doi:10.1016/j.watres.2011.08.007
- Warneke, S., L. Schipper, M. Matiasek, K. Scow, S. Cameron, D. Bruesewitz, and I. McDonald (2011b). Nitrate removal, communities of denitrifiers and adverse effects in different carbon substrates for use in denitrification beds. *Water Research* **45** (2011): pg.5463-5475. doi:10.1016/j.watres.2011.08.007
- Watanabe, T., H. W. Jin, K. J. Cho, and M. Kuroda (2004). Application of a bio-electrochemical reactor process to direct treatment of metal pickling wastewater containing heavy metals and high strength nitrate. *Water Science and Technology* **50** (8): pg.111-118.

- Water Sanitation and Health (2001). Water-related diseases. Available at: http://www.who.int/water_sanitation_health/diseases-risks/diseases/scabies/en/. Accessed 24 September 2016
- WHO (2006). *Guidelines for Drinking-Water Quality*. World Health Organization.
- Wrighton, K., B. Virdis, P. Clauwaert, S. Read, R. Daly, N. Boon, Y. Piceno, G. Andersen, J. D. Coates, and K. Rabaey (2010). Bacterial community structure corresponds to performance during cathodic nitrate reduction. *International Society for Microbial Ecology* **4** pg.1443-1455. doi:10.1038/ismej.2010.66
- Zhang, X. G., and W. R. Revie (2011). Galvanic Corrosion. In *Uhlig's Corrosion Handbook 3rd ed.*
- Zumft, W. G. (1997). Cell Biology and Molecular Basis of Denitrification. *Microbiology and Molecular Biology Review* **61** (4): pg.533-616.